RATES OF DIFFUSION-CONTROLLED ADSORPTION PROCESSES

RATES OF DIFFUSION-CONTROLLED ADSORPTION PROCESSES

by

George Rudolph Stifel, B.Ch.E.

A Thesis

Submitted to the Faculty of Graduate Studies

in Partial Fulfilment of the Requirements

for the Degree

Master of Engineering

McMaster University,

October, 1966

MASTER OF ENGINEERING
(Chemical Engineering)

McMASTER UNIVERSITY,
Hamilton, Ontario.

TITLE : Rate of Diffusion-Controlled Adsorption Processes

AUTHOR : George Rudoph Stifel, B.Ch.E.
(University of Detroit)

SUPERVISOR : Professor Robert B. Anderson

NUMBER OF PAGES : (xiv), 149

SCOPE AND CONTENTS :

Rate of adsorption data for gases on molecular sieves and coals have been interpreted using equations for unsteady state diffusion derived from Fick's law for spheres usually ignoring the amount adsorbed and the shape of the adsorption isotherm. These inappropriate equations result in calculated diffusivities that are too low and activation energies that are too large.

Numerical solutions of Fick's law were made for diffusion and adsorption in a porous sphere of radius R by finite difference methods for the following conditions:

a. Diffusion is the rate-controlling step, and the diffusivity, D, is constant.

b. Within an increment of the particle the total amount of adsorbate per unit volume, T is related to the "effective" concentration, C, by a Langmuir-like isotherm $T = abC/(1 + bC)$.

c. At zero time the particle containing no adsorbate is surrounded by adsorbate of concentration, C_o, which remains constant throughout

the rate process, and

d. Equilibrium is established immediately at the periphery of the sphere.

The solutions are obtained in terms of $Z = Q/Q_\infty$ and $\tau = (DC_o/Q_\infty R^2)t = kt$, where t is time, k is a constant equal to the term within the brackets, and Q and Q_∞ are the amounts adsorbed per unit volume at time t and at equilibrium. The quantity within brackets is also a valid expression for linear and Freundlich-like adsorption isotherms and probably holds for other isotherms. Plots of Z as a function of τ shift systematically as the parameter $B = bC_o$ increased from 0, corresponding to a linear adsorption isotherm, to large values; the value of Z at a given τ increasing with increasing values of B. For B = 0 the numerical solution is identical with analytical solution for the linear adsorption isotherm which for values of Z <0.87 is given by

$$kt = (2/\pi) \{(1 - \pi Z/6) - (1 - \pi Z/3)^{1/2}\}$$

where $k = DC_o/R^2Q_\infty$. For large values of B the numerical solutions approach as a limit the parabolic law

$$kt = (1/2) \{(1 - 2Z/3) - (1 - Z)^{2/3}\}$$

The value of $(1/k^{1/2})\, dZ/dt^{1/2}$ at short times increases from 3.385 for B = 0 to 4.243 for very large values of B. From experimental data the value of k derived using the equation for B = 0 is 1.56 larger than for the parabolic equation. Hence the values of D obtained from the initial linear portions of the rate curve change by only a factor of 1.56 when the type of isotherm is changed from linear to rectangular.

Rates of adsorption and the adsorption isotherm were determined for N_2, CH_4, CO_2, and C_2H_6 on samples of Linde 4A molecular sieve at several temperatures from -78° to $+50^\circ$C in a manostatic volumetric

adsorption apparatus. The Langmuir equation satisfactorily approximated the isotherms and the values of B were moderately large at the lower temperatures of each series of experiments, eg., for N_2 at $-78^{\circ}C$, 10.6; for CH_4 at $-78^{\circ}C$, 7.3; for CO_2 at $0^{\circ}C$, 64; for C_2H_6 at 0° and $30^{\circ}C$, 37 and 10.3.

The rate data plotted as Z against $t^{\frac{1}{2}}$ were not linear at short times but curved upward initially before becoming linear. The initial nonlinear portion persisted significantly longer than the brief uncertain period at the beginning of the experiment. This phenomena could result from the equilibration at the periphery of the particles requiring a finite time rather than being instantaneous.

An equation based on the parabolic law model and a first order equilibration process was derived, which fits the experimental data for $0.05 < Z < 0.95$. This equation is appropriate only to data with a large value of B, but is probably a reasonable approximation for other rate data.

The rates of adsorption for different molecules were $CO_2 > N_2 > CH_4 > C_2H_6$. The activation energies for the diffusivity were found to be 4.1 and 6.0 kcal./mole for methane and ethane. The heats of adsorption were found to be 7.2 and 8.3 kcal/mole for methane and ethane.

ACKNOWLEDGEMENTS

The author would like to acknowledge the assistance of those who contributed to this research. He is especially grateful to:-

His Research Director, Dr. Robert B. Anderson, whose guidance and enthusiasm were invaluable.

Linde, Division of Union Carbide for supplying the samples.

The National Research Council for their financial assistance.

Dr. A.E. Hamielec for able assistance in developing the computer programme used in the numerical solutions.

Mr. R.J. Palmer and his staff of the McMaster University Glassblowing shop for the fabrication of the adsorption apparatus used in this project.

Mr. R.W. Dunn of the Chemical Engineering Department for his assistance in fabrication and installation of equipment.

Dr. John Freel, who carried out the electron microscope studies of the aluminosilicates.

Mrs. S. Gravestock for her competent typing of the thesis.

His wife, Janice Ann Stifel, whose encouragement and patience made this work possible.

TABLE OF CONTENTS

LIST OF TABLES

LIST OF FIGURES

INTRODUCTION

When a gas or vapour comes into contact with an evacuated solid, a part of the gas is adsorbed by the solid, which in this case is an alumino-silicate. If this occurs at constant volume, the pressure drops; if at constant pressure, the volume decreases.(1) The amount of gas or vapour adsorbed is a function of both the adsorbent and adsorbate besides temperature and pressure. Therefore, the physical structure and the chemical composition of the alumino-silicate must be considered. Other important adsorbent properties are surface area, shape and distribution of pores. For molecular sieves we consider the volume of gas adsorbed and the crystal structure with its aperture size.(2)

If a gas enters the solid, the gas may adsorb or it may react with the solid and form a compound. If a gas remains attached to the surface of the solid, there is either a weak interaction between solid and gas, similar to condensation or a strong interaction, similar to chemical reactions. The former is called physical adsorption, the latter chemisorption and we are concerned with the former.(1) The molecules or atoms of the solid are held together by different forces: electrostatic, homopolar valence, van der Waals forces, etc. In most solids more than one are present with one predominating : in ionic crystals the electrostatic forces are most important while in atomic lattices the homopolar binding forces are. An atom located inside the body of the solid is subjected to equal forces in all directions,

whereas one at the surface is subjected to unbalanced forces. This results in a tendency to decrease the surface (a solid has surface tension). An atom or a molecule of gas adsorbed by the solid saturates some of the unbalanced forces thereby decreasing the surface tension. All adsorption phenomena are spontaneous and result in a free energy decrease of the system.(1)

The adsorption process is also accompanied by a decrease in entropy as a molecule on the surface now has fewer dimensions of freedom as compared to the three dimensions of freedom in the gaseous phase. The change in enthalpy is negative since both ΔF and ΔS are negative and $\Delta H = \Delta F + T\Delta S$. Therefore all adsorption processes are exothermic. This decrease in enthalpy is called the heat of adsorption. In van der Waals adsorption, it has the same order of magnitude as heats of condensation of gases, and in chemisorption as the heats of reactions.(1)

There are three methods of representing equilibrium adsorption data - the adsorption isotherm, the adsorption isobar and the adsorption isostere. Generally, the amount of gas adsorbed is a function of the final pressure and the temperature.(2)

When the pressure of the gas is varied at constant temperature, the plot of amount adsorbed as a function of the pressure is called the adsorption isotherm. Several observations can be made regarding this plot. At constant temperature the adsorption of a gas increases with increasing pressure. The amount of material adsorbed at equilibrium must always decrease with increasing temperature since the adsorption process is exothermic.

At small total adsorptions, the volume of adsorbed gas often increases linearly with pressure, obeying Henry's law,

$$v = Kp \tag{1}$$

where v is the volume adsorbed and p is the pressure. At higher total adsorptions the isotherms become parabolic and follow an equation known as the Freundlich isotherm equation

$$v = K'p^{1/n} \tag{2}$$

where $n>1$. At still higher total adsorptions, the volume adsorbed increases only slightly with pressure and saturation is attained. In this region

$$v = K'' \tag{3}$$

Isotherms with such shapes are called Langmuir isotherms.(1)

The adsorption isobar is a plot of the amount of gas adsorbed at equilibrium as a function of temperature at constant pressure.(2)

The adsorption isostere is a plot of the equilibrium pressure as a function of temperature at constant amount adsorbed and are convex with respect to the temperature axis. This plot is similar to a vapour pressure curve. For systems at equilibrium the Clapeyron-Clausius equation can be used to evaluate the heat change involved from one phase to another.

$$\left(\frac{\partial \ell n p}{\partial(\frac{1}{T})}\right)_Q = - \frac{q \text{ iso}}{R} \tag{4}$$

where q_{iso} is the isosteric heat of adsorption. The differential heat of adsorption is,

$$q_{diff} = q_{iso} - RT \qquad (5)$$

where R is the gas constant. The slope of a plot of ℓnp against 1/T gives the isosteric heat of adsorption[1].

Rates of adsorption may be limited by the process at the surface or as in the present case by diffusion into the porous solid. Generally Ficks' law describes the rate of diffusion, and for unsteady-state diffusion processes, i.e., where the concentration at a given point is a function of time, is given by[6].

$$\frac{\partial T}{\partial t} = D \frac{\partial^2 C}{\partial x^2} \qquad (6)$$

which applies to an infinite plate. Here C is the effective concentration, cc gas(STP)/cc., T is the total concentration cc(STP)/cc, t is the time in seconds and D is the diffusion coefficient, cm^2/sec.

2. SYSTEM STUDIED

The adsorption of Nitrogen, Carbon dioxide, Methane and Ethane are studied experimentally on Type 3A and Type 4A Molecular Sieves. Rate curves are determined at different temperatures on a modified B.E.T. apparatus.

Secondly, a numerical solution of Fick's law with Langmuir isotherm will be obtained for different values of B which equals bC_o where b is a constant and C_o is the initial concentration in the gas phase, cc/(STP)/cc. This solution is done on an IBM 7040 computer.

3. LITERATURE REVIEW

Zeolite minerals were discovered and named by Baron Cronstedt in 1756. These zeolites are the minerals that are now termed crystalline alumino-silicates or "molecular sieves".

The initial investigations on naturally occuring zeolites were performed in 1840 by Damour who reported on the reversible dehydration of the zeolite minerals. Damour also noted that the transparency and crystal form did not change on heating. Subsequently, other investigators studied the naturally occuring zeolites-chabazite, heulandite and analcite, which are part of a larger group of known and catalogued zeolites[2][7].

In 1925, Weigel and Steinhoff reported that the zeolite chabazite adsorbed water vapour, methyl and ethyl alcohol, but acetone and benzene were largely excluded. This is perhaps the first report of the molecular sieve behavior of crystalline zeolites. For a review of the early literature, the reader is referred to Barrer[7] and Hersh[2].

After 1925, extensive study yielded much information about the nature of zeolite materials but the properties of ion exchange, the reversible gain and loss of water and the adsorption of gases remained hidden. By this time, a concept of a sponge-like structure had been visualized. The application of x-ray diffraction techniques by Pauling and Taylor in the early 1930's led to the determination of the crystal structure of analcite and natrolite[8]. A list of some typical zeolites can be found in Barrer's paper[7]. The porous structure of

of zeolite crystals attracted the attention of some physical chemists, in particular, R.M. Barrer, who reported the results of his studies of the sorption of gases on chabazite and analcite[9].

Like all silicates, zeolites are built by the union of SiO_4 tetrahedra through sharing one or more oxygen atoms with neighbouring tetrahedra. Some SiO_4 tetrahedra are replaced by AlO_4 tetrahedra, thereby importing a negative charge to the framework, which is neutralized by an electrochemical equivalent of interstitial cations. The resulting structure is sufficiently open to enmesh interstitial water molecules, and upon this property depends their behavior as adsorbents[7].

On heating, zeolites lose their water with a variable degree of lattice shrinkage which is a minimum with the type we are interested in, or it may be large, or even amount to irreversible lattice collapse, in the case of the laminar or fibrous zeolites[9]. The non-collapsing zeolites are the most important, for not only are they capable of regaining their crystal water but sometimes adsorb other gases and vapours than water.

Typical isotherms, isobars and isosteres are found throughout literature[9][10][11]. The most successful of the equations describing isotherms are based on kinetic or statistical models[7] and have the form

$$\theta = \frac{bp}{1+bp} \qquad (7)$$

where θ denotes the fraction of all available interstices occupied by adsorbed molecules, p is the equilibrium pressure and b is a constant.

Attempts have been made by Weigel and others to obtain the

saturation values for adsorption in zeolites and are summarized by Barrer[7].

Heats of adsorption in zeolites have been measured directly and by the use of the Clapeyron equation. These heats do not differ significantly where both methods have been used on the same sample[7].

The power of a zeolite to adsorb not only depends upon the basic structure but also upon the severity and duration of the heating and degassing treatment before adsorption of a particular molecule. These factors determine the degree of lattice collapse or alteration. A maximum adsorption often occurs at about 95% dehydration, and after this point enough water will have been removed to lead to severe lattice collapse[7][12].

The kinetic behavior of adsorbates in zeolites has been interpreted as a pure diffusion process. As a diffusion process, adsorption rates follow Fick's law and the plots of volume adsorbed against time has been the most successful in interpreting the kinetic behavior[13]. The unsteady state molecular flow of small volumes of gas from zeolites under thermal conditions unfavourable to adsorption were studied by Nelson and Walker[14].

The type of equations used by previous workers were algebraic in form and applied only to linear adsorption. They ignored physical adsorption. Therefore, they obtained erroneous values for the activation energy and the diffusion coefficient. In their calculations for example they determined the quantity D/R^2 when the quantity should be D/aR^2, where a is a constant of physical adsorption.

The factors affecting diffusion and physical adsorption of gases include the polarizing power of the interstitial cation, the polarizability of the adsorbed molecule, the dimensions and shape of the sorbed molecule relative to the interstitial channels, duration and severity of heating and evacuation and the presence of foreign molecules in the iterstitial channels. Diffusion rates are also affected by the amount of sorbate adsorbed and on the state of subdivision of the crystals[15].

Synthesis of zeolite crystals were attempted with partial success. The majority of these accounts must be discredited due to improper identification[16][17]. Of these, the most successful synthesis of zeolite crystals were undertaken by Barrer[11][16][17]. Following Barrer, Milton and his associates at the Union Carbide Corporation's Linde Division, initiated a study of zeolite synthesis and by 1952, many different species of synthetic zeolites had been prepared[18]. Some were analogues of natural zeolites and the rest were new varieties of which one was designated Type A, with which we are concerned.

4. SCOPE OF THIS WORK

The scope of this work is to study the adsorption of hydrocarbons on molecular sieves and to interpret the rate data according to Fick's law. This will involve measuring rate curves and equilibrium isotherms at different temperatures. Also, numerical solutions of Fick's law for non-linear isotherms will be computed using finite difference methods for a sphere, a cylinder and a platelet.

5. EXPERIMENTAL

5.1 Volumetric Gas Adsorption Apparatus

The equipment is of glass construction (Figure 1) and is based on the B.E.T. Apparatus[5]. Referring to Figure 2, the system consists of an adsorption bulb (A), a bulb gas burette (B), a levelling bulb (C), a reversible 3 rpm motor (D), a graduated burette in 0.10 ml. divisions (E), a trap (F), an automatic device for maintaining constant pressure[6], a manometer (H) and a McLeod Gauge (J).

The adsorption bulb (A) contains the sample which is to be exposed to the adsorbate. The gas burettes (B) and (E) contain the majority of the adsorbate and through volume changes can increase or decrease the pressure in the system which is read on the right leg of manometer (H) when the mercury column is zeroed at the top electrode[6] in the left leg of the manometer. Trap (F) prevents oxygen or other gases which may diffuse through the tubing connected to the levelling bulb (C), from entering the system and affecting experimental results. If gas does accumulate in (F), it may be released through the stopcock (S5) to the atmosphere. The manostatic control (G) controls a reversible motor (D) which in turn controls the height of the levelling bulb (C) by making or breaking a circuit through two electrodes[6] with a mercury column in the left leg of the manometer (H). To compensate for gas removed from the burette system by adsorption, the levelling bulb rises when the circuit is made with the mercury column and the top electrode. Mercury is forced up into (E) by the rising levelling bulb which forces the

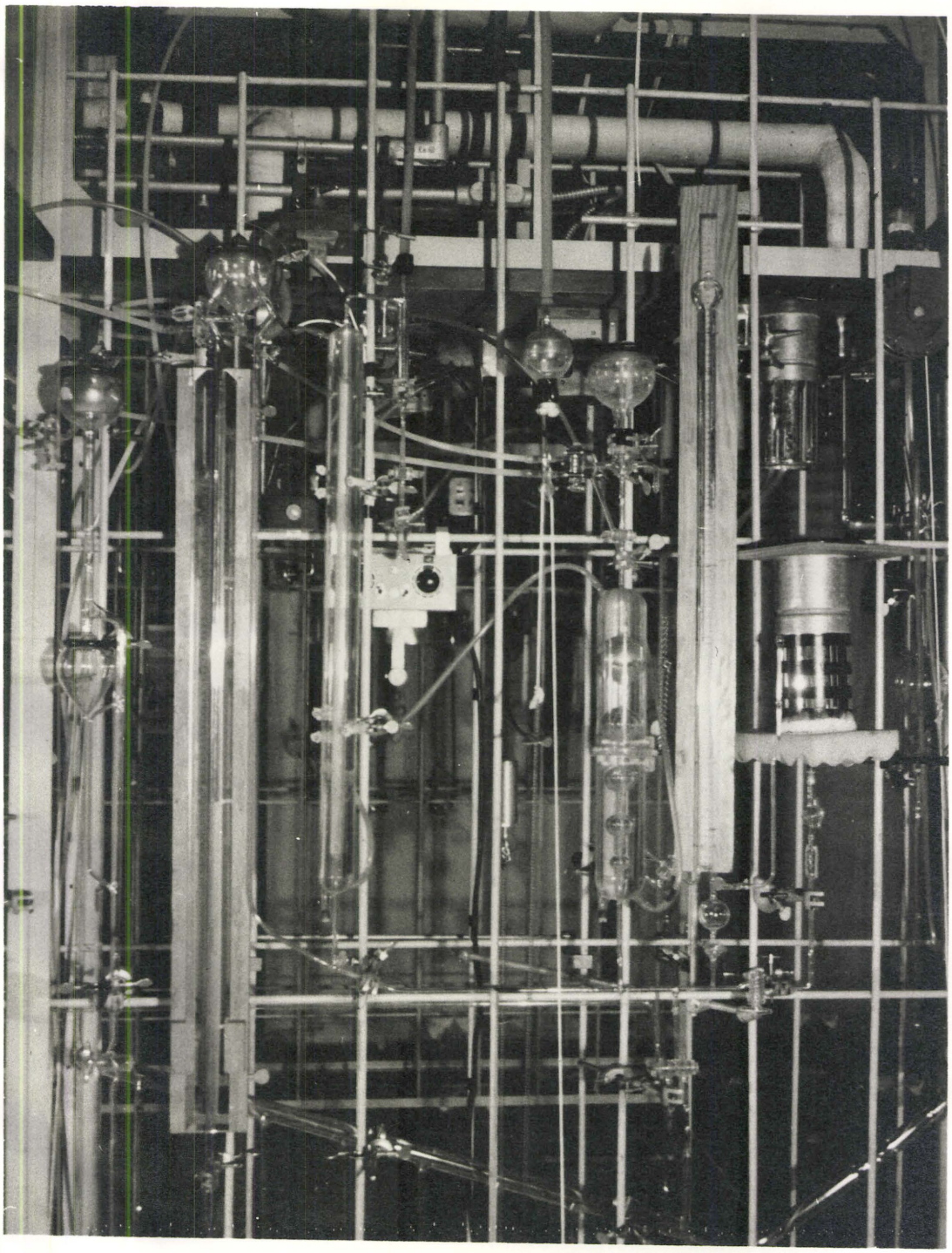

FIGURE 1 : Volumetric Gas Adsorption Apparatus

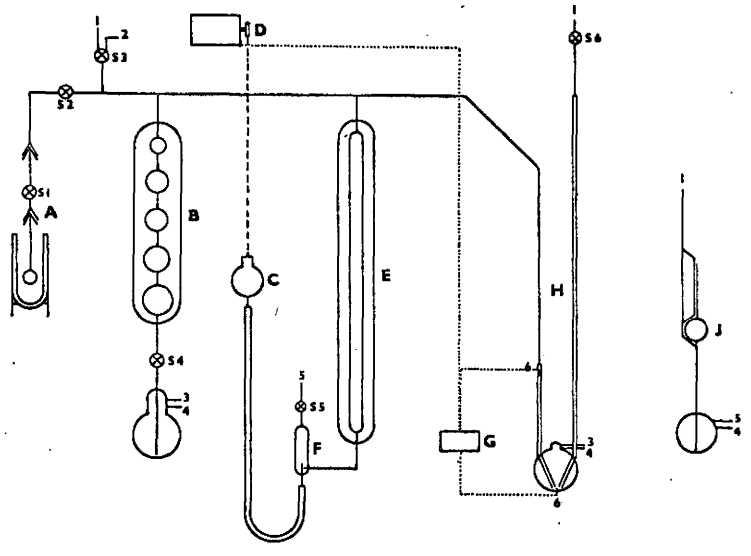
VOLUMETRIC GAS ADSORPTION APPARATUS
A
B
C
D
E
F
G
H
J
S1
S2
S3
S4
S5
S6

FIGURE 2

the gas in the system to push the mercury down in the left leg of the manometer. This breaks the circuit and keeps the pressure constant. The reverse is true when gas is entering the burette system as in desorption and in this case because the circuit is broken, the levelling bulb is lowered until the circuit is made. A McLeod Gage (J) is included in the system to check the vacuum obtained prior to introducing a gas into the system. It is connected to the vacuum manifold (not shown) which is in turn connected to the volumetric gas adsorption system. A vacuum of at least 10^{-6} torr is obtained with a mercury diffusion pump in series with a rotary vacuum pump.

The temperature of the adsorption bulb is kept constant by immersion in a dewar flask containing the appropriate thermostatted liquid. Both burettes have water jackets therefore the majority of the gas is kept at a temperature of 30°C.

Line (1.) leads to the high vacuum manifold, line (2.) leads to the gas storage system, line (3.) is connected to a 20 psig air source while line (4.) is connected to a low vacuum source and (5.) leads to the atmosphere. Through (3.), (4.) and (5.), the various reservoirs of mercury can be evacuated or pressurized.

5.2 ANALYTICAL

This section concerns itself with the various calibrations, zeolite structure, commercial description of the sieves and pretreatment and the gases involved.

5.2.1 CALIBRATION OF VOLUMETRIC GAS ADSORPTION APPARATUS

5.2.1.1 BURETTE CALIBRATION

Burette calibrations were made with double-distilled mercury at 30°C. For the five bulb burette (B), the volume was calculated from the weight of mercury emptied from each bulb. The calibration data for burette (B) are shown in Table 1. The 100 ml. tube burette (E) was calibrated with mercury at 30°C and found to be accurate within ±0.3%.

5.2.1.2 VOID SPACE DETERMINATION

The void space, V_v is the volume contained in the system to the right of S1 and below S2 (Figure 2) which is not accounted for by the burettes. This void space determination is carried out with nitrogen or helium. A fixed amount of gas is introduced into the system and widely separated pressures are recorded with their corresponding calibrated volumes. By application of the Ideal Gas Law, the volume of the void space was determined.

5.2.1.3 DEAD SPACE FACTOR

The dead space factor, F_c, accounts for the space in the adsorption bulb up to S2, (Figure 2). Helium is used to determine F_c because helium is not usually adsorbed on most solids, though this may not be true for molecular sieves. This assumption is justified for most solids because at adsorption temperatures of 77°K or higher, helium

TABLE 1:

BULB VOLUMES OF GAS BURETTE (B)

BULB	V,cc
1	4.60
2	16.31
3	22.76
4	49.42
5	135.06
Total	228.15

adsorption will always be small compared to that of the adsorbate used[4].

The dead space factor, F_c, the STP volume of gas entering the dead space per unit pressure is

$$F_c = \frac{\Delta V(STP)}{P} \qquad (8A)$$

where $$\Delta V = Q + \frac{VP}{T}\,\frac{273}{760} + \frac{vP}{300}\,\frac{273}{760}$$

P = pressure, mm Hg.

V = volume in thermostatted bath

v = volume at room temperature (300°K)

T = Temperature °K of volume in thermostatted bath

Q = Amount adsorbed cc(STP)/g.

Therefore:

$$F_c = \frac{Q}{P} + \left(\frac{V}{T} + \frac{v}{300}\right)\frac{273}{760} \qquad (8B)$$

It is reasonable to assume that if helium is adsorbed in significant amounts, the isotherm will be linear, i.e. Q/P is a constant at a given temperature. Q/P is strongly temperature dependent and decreases rapidly with increasing temperature. Equation (8B) at higher temperatures becomes

$$F_cT = \frac{273}{760}\left(V + \frac{vT}{300}\right) \qquad (8C)$$

The values on a FT versus T plot for -78°C and higher fall on a straight line. Therefore F_c can be extrapolated to for lower temperatures to give a reasonable estimate.

Helium is allowed to enter the system to the right of S2 (Figure 2). The initial volume of gas is determined and the gas is then allowed to enter the adsorption bulb at a specified temperature. Three readings

at widely separated pressures are recorded with their corresponding burette volumes, Vc and the void space, V_v to determine the amount of gas left to the right of S2 (Figure 2). These volumes of gas are subtracted from the initial volume of gas and the differences are divided by their respective pressures to give F_c. An average value of F_c is then taken and a plot of F_cT versus T is made. The points at -79°C and higher all fall on a straight line. The dead space factor for -195°C is extrapolated from the points at the higher temperatures. There is a difference between the measured value at -195°C and the extrapolated value, for example for one sample, 0.19997 for the former and 0.18694 for the latter. The extrapolated value is taken as the correct one. Table 2 shows the dead space factors at their respective temperatures for a typical sample.

Nitrogen at -195°C and carbon dioxide, methane and ethane at -79°C are not ideal gases. Therefore a correction factor, α, must be introduced to account for the non-ideality and through the use of equation (8D).

$$F_c' = F_c(1+\alpha P) \qquad (8D)$$

the dead space factor can be corrected. P here is in atmospheres and F_c' is the corrected dead space factor. Table 3 gives the corrections, α, for the individual gases.

For the volume usually involved in the dead space, it is not necessary to correct except for Nitrogen at -195°C.

TABLE 2

DEAD SPACE FACTORS, 4A COMPRESSED POWDER

Temperature, °C	F_c
30°	0.08202
0°	0.08762
-78°	0.09851
-195°	0.18694

TABLE 3

NON-IDEALITY CORRECTION FACTORS AT 1 ATM

Gas	Temperature	α, %
N_2	-195°	5.00
CO_2	-78°	2.09
CH_4	-78°	1.30
C_2H_6	-78°	3.30

5.2.2 TYPE A MOLECULAR SIEVE

5.2.2.1 ZEOLITE STRUCTURE

The zeolites are a group of hydrated silicates which have similar compositions and properties[2][7]. The composition of zeolites includes SiO_2, Al_2O_3, a cation or cations to balance the negative change of the alumina-silicate structure and water of hydration. The most common cations are sodium and calcium. The alumino-silicate can be represented by the formula

$$(R,R'_2)\ O\ ,\ Al_2O_3,\ nSiO_2,\ MH_2O$$

where R = Ca, Sr, and Ba and R' = Na,K. The ratio of base to Al_2O_3 is always 1:1 and the ratio (Al + Si):O = 1:2. These minerals are widespread but massive deposits are usually not found. They are formed under comparatively alkaline and probably stagnant conditions by hydrothermal alteration of older rocks and lavas at temperatures between 100° and 350°[7].

The structures of many zeolites consist of simple arrangements of polyhedra where each polyhedran is a three-dimensional array of (Si, AlO$_4$) tetrahedra in a definite geometric form. In the structure of zeolite Type A, the octahedra are linked in a cubic array by joining with cubes in the square faces (Figure 3). A central truncated cube octahedron with an internal cavity of 11Å in diameter is formed. This central cavity is entered through six circular apertures formed by a nearly regular ring of eight oxygens with a free diameter of 4.2Å. The cavities are arranged in a continuous three-dimensional pattern with a system of unduloid-like channels with a minimum diameter of 4.2Å and a maximum of 11Å. These truncated

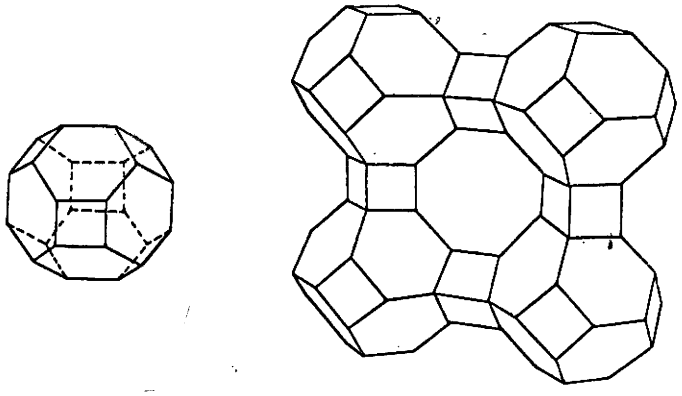

FIGURE 3 The Archimedean truncated octahedron (left) and the simple cubic array of truncated octahedra in the zeolite type A (right).

octahedra themselves enclose a second set of smaller cavities (6.6Å internal diameter) and are connected to the larger cavities by a distorted ring of six oxygen atoms with a 2.2Å free diameter. Therefore in each crystallographic unit cell of zeolite Type A, there are 12 AlO_4 and 12 SiO_4 tetrahedra and therefore, 12 monovalent cations (Na^+). Eight of the sodium ions lie in the center of the six rings in the hexagonal faces and four occupy positions adjacent to the eight ring. When the zeolite is hydrated, the four sodium ions are probably completely hydrated and float in the center of their co-ordination sphere of water molecules. When the zeolite is dehydrated, the cations are found to locate on the cavity walls since in structural analysis, short Na-O distances are usually found. The eight Na^+ ions in the six rings are classified as Type I and the remaining four as Type II[8].

5.2.2.2 ADSORPTION DATA SHEETS FOR TYPE 3A and TYPE 4A

5.2.2.2.1 Linde Molecular Sieve - Type 3A

Description

Molecular Sieve Type 3A, the potassium form of the Type A crystal structure, is an alkali metal alumino-silicate. Type 3A will adsorb molecules with critical diameters up to 3 angstroms.

Applications

Type 3A is the preferred Molecular Sieve adsorbent for the commercial dehydration of unsaturated hydrocarbon streams such as cracked gas, propylene, butadiene, and acetylene. It is also used for drying polar liquids such as methanol and ethanol.

The small pore size of Type 3A prevent coadsorption of hydrocarbons by excluding all other molecules while adsorbing water.

Chemical Formula

$$K_9Na_3[(AlO_2)_{12}(SiO_2)_{12}] \cdot 27\ H_2O$$

Typical Properties

Nominal Pore Diameter	3 angstroms
Available Form	Powder 1/16-in. Pellets 1/8 -in. Pellets
Bulk Density	
Powder	30 lb/cu.ft.
1/16-in. pellets	47 lb/cu.ft.
1/8 -in. pellets	47 lb/cu.ft.
Particle Diameter	
1/16-in. pellets	0.0575 in. to 0.0775 in.
1/8 -in. pellets	0.115 in. to 0.135 in.

Crush Strength
1/16-in. pellets ..... 6.4 lbs.
1/8 -in. pellets .....14.5 lbs

Crystal Form ..... Cubic

Heat of Adsorption (max.) ..... 1800 btu/lb H_2O

Equilibrium H_2O Capacity*
Powder ..... 23% wt
1/16-in and 1/8 in. pellets ..... 20% wt

Water Content (as shipped) ..... <1.5% wt

Molecules Adsorbed ..... Molecules with an effective diameter <3 angstroms, including $H_2O$and NH_3

Molecules Excluded ..... Molecules with an effective diameter >3 angstroms, e.g. ethane

---

* Lbs. H_2O/100 lbs activated adsorbent at 17.5 mm Hg, 25°C

Regeneration

Molecular Sieve Type 3A can be regenerated for re-use by heating, with simultaneous purge, or by evacuation. Water can be removed by heating the material at 475°F. (Repeated exposure to purge gas containing H_2O at higher partial pressure or at bed temperature of 800-1000°F should be avoided.) The degree of regeneration (water removal) is dependent on the temperature and humidity of the purge gas.

In liquid phase operation, all liquid should be drained from the Molecular Sieve before regeneration. Reverse flow is advantageous in all regenerations.

5.2.2.2.2 Linde Molecular Sieve - Type 4A

Description

Molecular Sieve Type 4A, the sodium form of the Type A crystal structure, is an alkali metal alumino-silicate. Type 4A will adsorb molecules with critical diameters up to 4 angstroms.

Applications

Type 4A is the preferred Molecular Sieve adsorbent for static dehydration in a closed gas or liquid system. It is used as a static desiccant in household refrigeration systems; in packaging of drugs, electronic components and perishable chemicals; and as a water scavenger in paint and plastic systems. Type 4A is also used commercially in drying saturated hydrocarbon streams.

All molecules which can be adsorbed on Molecular Sieve Type 3A can be adsorbed on Molecular Sieve Type 4A

Chemical Formula

$$Na_{12}[(AlO_2)_{12}(SiO_2)_{12}] \cdot 27\ H_2O$$

Typical Properties

Nominal Pore Diameter ..... 4 angstroms

Available Form ..... Powder
1/16-in. and 1/8-in Pellets
8 x 12 and 4 x 8 Beads
14 x 30 Mesh

Bulk Density
Powder ..... 30 lb/cu.ft.
1/16-in and 1/8-in pellets ..... 45 lb/cu.ft
8 x 12 and 4 x 8 beads ..... 45 lb/cu.ft
14 x 30 mesh ..... 44 lb/cu.ft.

Particle Diameter
1/16-in pellets ..... 0.0575 in. to 0.0775 in.
1/8 -in pellets ..... 0.115 in. to 0.135 in.
8 x 12 beads .....0.0661 in. to 0.0937 in.
4 x 8 beads ..... 0.0937 in. to 0.187 in.
14 x 30 mesh ..... 0.0232 in. to 0.0555 in.

Crush Strength	
1/16-in pellets	10.4 lb.
1/8 -in pellets	21 lb.
8 x 12 beads	6.9 lb.
4 x 8 beads	18 lb.
Crystal Form	Cubic
Heat of Adsorption (max.)	1800 btu/lb. H_2O
Equilibrium H_2O Capacity *	
Powder	28.5% wt.
1/16-in and 1/8-in pellets	22% wt.
8 x 12 and 4 x 8 beads	22% wt.
14 x 30 mesh	22% wt.
Water Content (as shipped)	< 1.5% wt
Molecules Adsorbed	Molecules with an effective diameter <4 angstroms, including ethanol, H_2S, CO_2, SO_2, C_2H_4, C_2H_6, and C_3H_6
Molecules Excluded	Molecules with an effective diameter <4 angstroms, e.g. propane

*Lbs H_2O/100 lbs. activated adsorbent at 17.5 mm Hg. 25°C

Regeneration

Molecular Sieve Type 4A can be regenerated for re-use by purging or evacuating at elevated temperatures. Water can be removed by heating the material at 400 to 600°F. (Repeated exposure to temperatures over 1100°F should be avoided). The degree or regeneration (water removal) is dependent on the temperature and humidity of the purge gas.

In liquid phase operation, all liquid should be drained from the Molecular Sieve before regeneration. Reverse flow is advantageous in all regenerations.

5.2.2.3 SAMPLE PRETREATMENT

The type 3A and 4A pelletized molecular sieve samples were intially dried in a convection oven at 250°C for 36 hours. They were then removed and placed into an adsorption bulb and evacuated at 250°C to 300°C for 4 to 6 hours. The adsorption bulb with sample was weighed before and after evacuation.

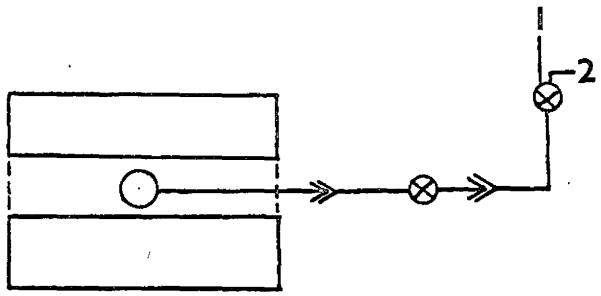

FIGURE 4: System for Evacuation of Sample Period
1 leadsto vacuum manifold
2 leads to atmosphere

Type 4A powder was hydrated for 22 hours and then placed into one inch moulds and compressed at 11,200 psig to 12,000 psig for two to three minutes to give a tablet which was then broken up. The sample was collected from the size range of 0.05 to 0.10 inch. It was then dried in air in an oven at 350°C for 36 hours. The sample was then placed in an adsorption bulb and the same procedure and equipment as for the Type 4A pellet is used.

The weight loss for the Type 4A pellet is 0.096% and for the Type 4A compressed powder is 0.010%.

5.2.2.4 ELECTRON MICROSCOPE EXAMINATION

The objective of the electron microscope examination of the Type 4A compressed molecular sieve was to determine the size and structure of the particles. A Siemens Elmiskop I electron microscope was used for this examination. The cubic particle in Figure 6 was taken as typical of six micrographs taken. The edge of the cube was found to be of the order of 2.5×10^{-5} cm. This value will be used for the diameter of the particle we are concerned with in the calculations to follow. Figure 6 shows the shapes resulting from cubes oriented in different positions.

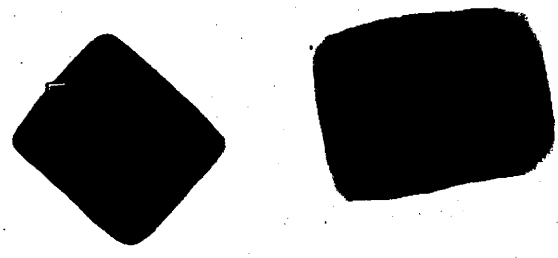

FIGURE 5:
Electron Micrograph of Type 4A Powder at 16,000 X.

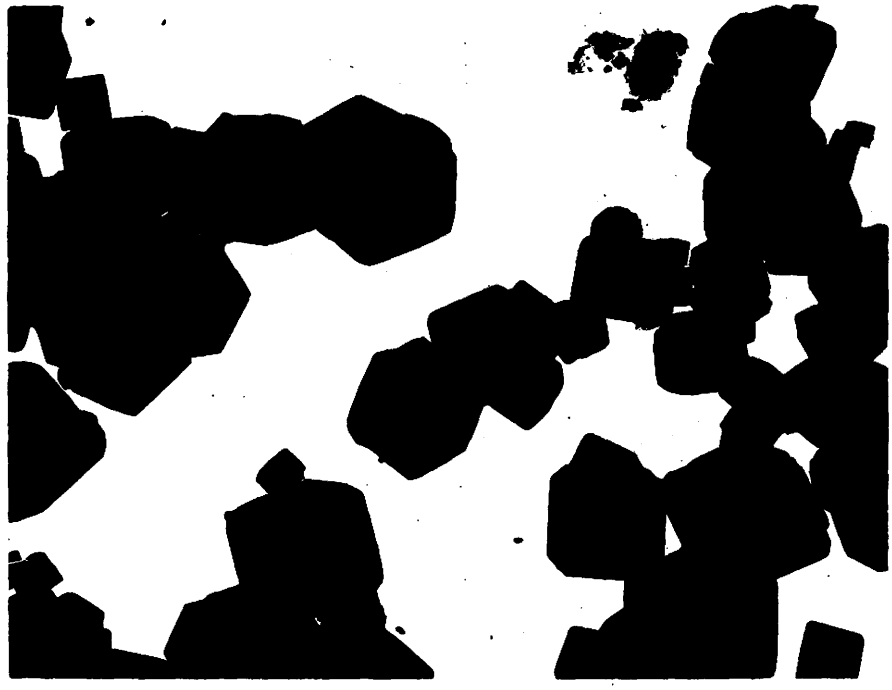

FIGURE 6:
Electron Micrograph of Type 4A Powder at 10,000X.

5.2.3 GASES

The gases used in this project were obtained from more than one source.

TABLE 4

SUPPLIERS OF GASES AND PURITY

Gas	Supplier	Purity, min.
He	Matheson Canada Limited	99.995%
N_2	Matheson Canada Limited	99.999%
CO_2	Canadian Liquid Air Limited	99.80%
CH_4	Matheson Canada Limited	99.99%
C_2H_6	Matheson Canada Limited	99.98%

All the gases were transferred into glass storage bulbs after being treated by passing through cold traps to remove any moisture which might have been present. The helium was passed through a trap filled with activated carbon and immersed in liquid nitrogen before entering the storage bulb. Nitrogen was passed first into a trap immersed in liquid hitrogen and allowed to condense. A quantity greater than needed is collected. The liquid nitrogen collected is then pumped to remove any lighter ends. It is then allowed to evaporate through a second trap immersed in liquid nitrogen to prevent any impurities from being carried into the gas storage system. Gases are stored at greater than one atmosphere. Also there is always some liquid left in the first trap which is then evaporated to the atmosphere.

Carbon dioxide, methane and ethane are also collected in a trap immersed in liquid nitrogen. The second trap is immersed in a dry ice-acetone bath and the procedure is the same as for nitrogen.

5.3 EXPERIMENTAL PROCEDURE

The particular method of operation for the volumetric gas adsorption apparatus constructed is to evacuate the burette system through stopcock S3 with S2 closed. After pretreatment of the sample (Section 5.2.2.3), the adsorption bulb (A) is connected to the system with S1 closed. S2 is opened and evacuation continues. When the McLeod Guage (J) shows at least 10^{-6} torr, S2 is closed and S1 is opened. The adsorbate is now introduced into the burette system through S3 and the quantity measured by pressure-volume relationship.

The timer and the manostatic control system (C), (D) and (G), are set at zero. The manostatic control system is zeroed by setting the mercury column in the left leg of the manometer (H) at the tip of the top electrode[6]. The right leg has been previously set at the desired pressure by appropriate changes in the volume of burettes (B) and (E). A constant temperature bath is placed around the adsorption bulb, (A) and the sample allowed to reach bath temperature.

The adsorption run is initiated by opening stopcock S2, which exposes the sample to the adsorbate, starting the timer and the manostatic control system. As gas is removed from the system by adsorption on the sample, the manostatic control system keeps the pressure constant by raising the levelling bulb (C). Readings are taken from burette (E) initially at half minute intervals and as the rate decreases, at longer intervals until equilibrium is reached.

For desorption, the procedure is the same except the S2 is opened to expose a previously equilibrated sample to a lower pressure. The manostatic control system is now set to operate when the circuit is broken and shut down when the circuit is completed. In this case, the levelling bulb is now lowered to keep the pressure constant, and desorption is followed.

6. NUMERICAL SOLUTIONS

6.1 COMPUTER PROGRAM

Numerical solutions of Fick's law for non-linear isotherms were computed using a finite difference method. The rate controlling factor is assumed to be the diffusion of the adsorbate into the porous material. The adsorption process is assumed to be instantaneous and to occur at constant temperature. The boundary conditions for a particle at zero time are: within the particle, the effective concentration, C = 0.0 and at the surface of the particle, C_o = 1.0. Finally the diffusivity, D, is constant.

Starting with the equation as formulated by Crank[4].

$$\frac{\partial T}{\partial t} = D \left[\frac{\partial^2 C}{\partial x^2} + \frac{\partial^2 C}{\partial y^2} + \frac{\partial^2 C}{\partial z^2} \right] \qquad (9)$$

where T is the total amount of adsorbate in the porous material, $cm^3(STP)/cm^3$, C is the effective concentration, $cm^3(STP)/cm^3$; t is the time in seconds and D is the diffusion coefficient. In pores of molecular dimension there is no need to distinguish between the molecules adsorbed and those in the gas phase. Therefore the total amount adsorbed, T, contains both quantities. T in this case is always greater than C. Equation (9) can be set up in general form to give

$$\frac{\partial T}{\partial t} = D \left[\frac{\partial^2 C}{\partial r^2} + \frac{n}{r} \frac{\partial C}{\partial r} \right] \qquad (10)$$

where n = 2 for a sphere, n=1 for a cylinder and n=0 for a platelet. For a sphere and cylinder, r is the radial position and for a platelet r becomes $\ell/2$, one-half the thickness.

Taking the case for the sphere, n=2, normalization is carried out by introducing x = r/R and y = C/C_o, where R is the particle radius

and C_o is the concentration at the surface. For the solution of Fick's law considered here, the adsorption isotherm is assumed to be of the Langmuir type[20].

$$T = \frac{abC}{1+bC} \tag{11}$$

Normalization gives

$$T = \frac{abC_o y}{1+bC_o y} \tag{12}$$

which when substituted into (10) gives

$$abc. \quad \frac{\partial\left[\frac{y}{1+bC_o y}\right]}{\partial t} = \frac{DC_o}{R^2} \left[\frac{\partial^2 y}{\partial x^2} + \frac{2}{x} \frac{\partial y}{\partial x} \right] \tag{13}$$

If a non-dimensional time T is introduced which equals tD/abR^2 and also $bC_o = B$ we arrive at

$$(1+By)^{-2} \quad \frac{\partial y}{\partial \tau} = \frac{\partial^2 y}{\partial x^2} + \frac{2}{X} \frac{\partial y}{\partial x} \tag{14}$$

Equation (14) is the basic equation in the computer program. Finite difference calculations will give y at different positions for a given T. From these values of y, we may calculate T in (12). Introducing Q as the total amount adsorbed to avoid confusion,

$$Q = 4 \Pi \int_o^R Tr^2 dr \tag{15}$$

and after substitution and normalization

$$Q = 4 \Pi abC_o R^3 \int_o^1 \frac{y}{1+bC_o y} x^2 dx \tag{16}$$

The amount adsorbed at equilibrium is

$$Q_\infty = \frac{abC_o}{1+bC_o} \qquad (17)$$

The fractional approach to equilibrium factors[21], Z, is simply the ratio Q/Q_∞. Therefore

$$Z = 3(1+bC_o) \int_0^1 \frac{y}{1+bC_o y} x^2 dx \qquad (18)$$

where again $bC_o = B$, for purposes of calculation and b is the value obtained from the Langmuir plot. The only requirement is that b be expressed in the same units as used in calculating C_o, i.e., cc(STP)/cc

Rearranging (14)

$$\frac{\partial y}{\partial \tau} = (1+By)^2 \left[\frac{\partial^2 y}{\partial x^2} + \frac{2}{X} \frac{\partial y}{\partial x} \right] \qquad (19)$$

The sphere is divided into 20 equally spaced shells and indexed from 0 to 21 starting at the centre. The following finite difference formulas[22] are applied to equation (19).

$$\frac{\Delta^2 y}{\Delta x^2} = \frac{y(I+1,1) - 2y(I,1) + y(1-1,1)}{(DX)^2} \qquad (20)$$

$$\frac{\Delta y}{\Delta x} = \frac{y(I+1,1) - y(I-1,1)}{2DX} \qquad (21)$$

DX here equals 1.0 divided by the number of increments into which the particle is divided minus 1. The equation arrived at for use in the computer program for a spherical particle is

$$y(I,2) = y(I,1) + DT(1.0 + By(I,1))^2 \left[(y(I+1,1)A1(1) + y(I-1,1)A2(I) - 2y(I,1)A3(I)\right] \quad (22)$$

where

$$A1(I) = \frac{1}{(DR)^2} \left[1.0 + \frac{1.0}{FLOAT(I-1)}\right] \quad (23)$$

$$A2(I) = \frac{1}{(DR)^2} \left[1.0 - \frac{1.0}{FLOAT(I-1)}\right] \quad (24)$$

$$A3(I) = \frac{1}{(DR)^2} \quad (25)$$

where FLOAT(I-1) is the number of radial increments minus one. The program as used is shown on the following page.

To change the program so it will apply to a cylinder or to a platelet, A1(I), A2(I) and the volume are the only terms affected.

For a cylinder:

```
A1(I) = (1.0/(DR*DR)) * (1.0 + 1.0/(2.0* FLOAT(I-1))

A2(I) = (1.0/(DR*DR)) * (1.0 - 1.0/(2.0* FLOAT(I-1))

DVOL  = 2.0 + 3.1416* (DR*FLOAT(I-1))*DR
```

and for a platelet

```
A1(I) = A2(I) = A3(I) = 1.0/(DR*DR)

DVOL  = DR
```

The program is run at different values of B from 0.0 to 99.0. The results are printed out as Z and as concentrations at different y's for a given T.

```
      1       DIMENSION Y(21,2),A1(21),A2(21),T(21,2)
      2       READ(5,113) B
      3       WRITE(6,114) B
      4       WRITE(6,115)
      5       READ(5,100) KRUN,NRINC
     10       WRITE(6,101) KRUN,NRINC
     11       WRITE(6,115)
     12       READ(5,104) DT,NPRINT,NINT
     15       WRITE(6,105) DT,NPRINT,NINT
     16       WRITE(6,115)
     17       LR=NRINC-1
     20       DR=1.0/FLOAT(LR)
C
C      CALCULATE COEFFICIENTS THROUGHOUT MESH
C
     21       DO 1 I=2,NRINC
     22       R=DR*FLOAT(I-1)
     23       A1(I)=(1.0/(DR*DR))*(1.0+1.0/FLOAT(I-1))
     24     1 A2(I)=(1.0/(DR*DR))*(1.0-1.0/FLOAT(I-1))
     26       A3=1.0/(DR*DR)
C
C      SET BOUNDARY AND INITIAL CONDITIONS
C
     27       DO 2 I=1,LR
     30     2 Y(I,1)=0.0
     32       Y(21,1)=1.0
     33       Y(21,2)=1.0
     34       T(21,2)=Y(21,2)/(1.+B*Y(21,2))
     35       TIME=0.0
     36       WRITE(6,111) TIME,(Y(I,1),I=1,NRINC)
     43       WRITE(6,115)
C
C      START MARCHING CALCULATIONS
C
     44       DO 4 K=1,NPRINT
     45       DO 7 KK=1,NINT
     46       TIME=TIME+DT
     47       DO 5 I=2,LR
     50       Y(I,2)=Y(I,1)+(DT*(1.0+B*Y(I,1))**2)*(Y(I+1,1)*A1(I)
     1+Y(I-1,1)*A2(I)-2.0*Y(I,1)*A3)
     5   T(I,2)=Y(I,2)/(1.0+B*Y(I,2))
     51       DO 6 I=2,LR
     53       T(I,1)=T(I,2)
     54     6 Y(I,1)=Y(I,2)
     55       Y(1,1)=Y(2,1)
     57       T(1,1)=T(2,1)
     60     7 CONTINUE
     61       WRITE(6,111) TIME,(Y(I,1),I=1,NRINC)
     63       Y(1,2)=Y(2,2)
     70       T(1,2)=T(2,2)
     71       BPASS=0.0
     72
```

```
  73          VØL=0.0
  74          DØ 15 I=2,NRINC
  75          DVØL=4.0*3.1416*((DR*FLØAT(I-1))**2)*DR
  76          VØL=VØL+DVØL
  77       15 BMASS=DVØL*(T(I,2)+T(I-1,2))/2.0 +BMASS
 101          Z=BMASS*(1.0+B)/VØL
 102          WRITE(6,112) Z
 103          IF(Z.GT.0.99999) GØ TØ 200
 106          WRITE(6,115)
 107        4 CØNTINUE
      C
      C       XXXXXXXXXXXXXXXXXXXXXXXXXXXXXXXXXXXXXXXXXXXXXXXXXXXXXXXXXXXXXXXXXXXXXXXXXXXXXXX
      C
 111     115 FØRMAT(/)
 112     100 FØRMAT(2I5)
 113     101 FØRMAT(7H RUN NØ,I5,3HFØR,I5,17HRADIAL INCREMENTS)
 114     104 FØRMAT(F10.5,2I5)
 115     105 FØRMAT(16H TIME INCREMENTS,F10.5,15HNØ ØF PRINTØUTS,I5,
            123HINCREMENTS PERPRINTØUT,I5)
 116     111 FØRMAT(8H TIME IS,F10.5/(1X,21F6.3))
 117     112 FØRMAT(5H Z IS,F10.5)
 120     113 FØRMAT(F12.3)
 121     114 FØRMAT(F14.4)
 122     200 STØP
 123         END
```

6.2 PARABOLIC LAW AND FICK'S LINEAR ISOTHERM

The values obtained from the computer program are plotted with those obtained from the exact solutions of the Parabolic Law[23], (FP), as the upper limit ($B = \infty$) and Fick's linear isotherm[4][21], (FLI), as the lower limit ($B = 0$). The exact solutions check the validity of the numerical solutions.

Weisz and Goodwin[23] postulate the following for the Parabolic Law: the adsorbate is strongly adsorbed, eg. if $Q = f(C)$ such as the Langmuir equation, then Q increases to its maximum value, Q_∞, at very low concentrations; the boundary conditions are the same as postulated for the numerical solution; and finally the ratio $Q_\infty/C_o = A$.

For spheres, the profiles of C and T for a given time are as shown in Figure 7.

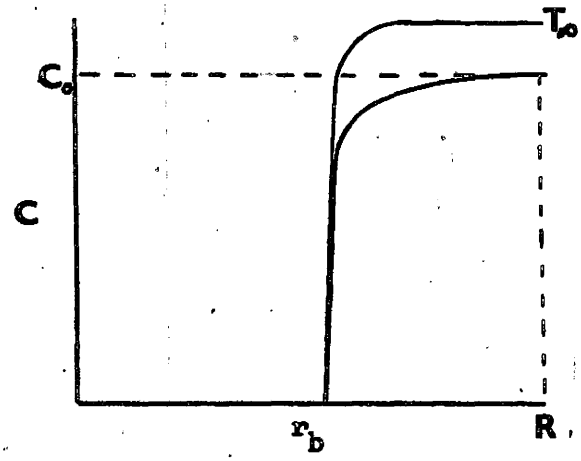

FIGURE 7 : C and T Profiles at a Given Time

where r_b is the radius at which T_∞ and C have decreased to zero and R is the radius of the particle. The layer occupied by the adsorbate ($r > r_b$) at essentially an amount T_∞, moves radially inward. From r_b to R, there is essentially no change in $\partial(C+T)/\partial t^*$ and

$$\frac{\partial^2 C}{\partial r^2} + \frac{2}{r}\frac{\partial C}{\partial r} = 0 \qquad (26)$$

then

$$\frac{\partial^2 Cr}{\partial r^2} = 0 \qquad (27)$$

and

$$\frac{\partial Cr}{\partial r} = K \qquad (28)$$

Integrating gives

$$Cr = Kr + J \qquad (29)$$

Applying the boundary conditions which are $C = C_o$ at $r = R$ and $C = 0$ at $r = r_b$, we get

$$C_o R = KR - Kr_b \qquad (30)$$

where $K = C_o R/(R-r_b)$. Therefore

$$\frac{\partial C}{\partial r} = C + r\frac{\partial C}{\partial r} \qquad (31)$$

Substituting for $\partial C/\partial r$, we arrive at the following equation at $r = R$.

$$R\left(\frac{\partial C}{\partial r}\right)_R = C_o\left(\frac{r_b}{R-r_b}\right) \qquad (32)$$

In the next step, taking Q_∞ so that $K = DC_o/Q_\infty R^2$ which will fall out in equation (36) and also considering the change in volume adsorbed as

$$\frac{dQ}{dt} = f\,4\pi R^2 D\left(\frac{\partial C}{\partial r}\right)_R \qquad (33)$$

* $t = T$, non-dimensional time

$$= 4\pi RC_o \left(\frac{r_b}{R-r_b}\right) \quad (34)$$

Dividing Q by Q_∞ to get Z

$$\frac{dZ}{dt} = \frac{4\pi DR}{\frac{4}{3}\pi AR^3} \left(\frac{r_b}{R-r_b}\right) \quad (35)$$

and also noting that $1-Z = (r_b/R)^3 = y$, we arrive at

$$(y^{-1/3} - 1)\, dy = -3\, \frac{D}{AR^2}\, dt \quad (36)$$

Integrating with respect to y and t and resolving the constant of integration with the boundary condition; t = 0, at y = 1. The final form is

$$\left(\frac{1-Z}{3}\right) - \frac{(1-Z)^{2/3}}{2} + \frac{1}{6} = Kt \quad (37)$$

Using a binomial expansion, the limiting form of equation (37) is shown to be, for small Z.

$$\frac{Z^2}{18} + \frac{2}{81} Z^3 = Kt \quad (38)$$

The limiting slope for (38) is $\partial Z/\partial t^{\frac{1}{2}} = 4.24\sqrt{K}$. Similar equations can be derived for the case of a cylinder and a platelet.

The exact equation of FLI for spheres [21] is

$$1 - Z = \left(\frac{6}{\pi^2}\right) \sum_{n=1}^{\infty} \left(\frac{1}{n^2}\right) \exp(-\pi^2 n^2 K_3 t) \quad (39)$$

where $K_3 = D/r^2$ and D is the Diffusivity and r is the radius of the sphere. The linear form is

$$(\pi Kt)^{\frac{1}{2}} = 1 - (1 - \frac{\pi Z}{3})^{\frac{1}{2}} \qquad (40)$$

and can be expanded for small values of Z into its limiting form

$$\frac{\pi Z^2}{36} + \frac{\pi^2 Z^3}{216} = Kt \qquad (41)$$

The limiting slopefor (40) is $\partial Z/\partial t^{\frac{1}{2}} = 3.39\ \sqrt{K}$. The simplest way to represent data of this type is with a plot of $Z/t^{\frac{1}{2}}$ verus $t^{\frac{1}{2}}$. This would fit if the experimental data comes directly from the origin. The plot gives a straight line for FLI but as B increases, the curvature increases slightly. In this case the curve can still be reasonably approximated by a straight line. FLI is exact to Z = 0.87 and is of the form

$$\frac{Z}{t^{\frac{1}{2}}} = K^{\frac{1}{2}}A - KBt^{\frac{1}{2}} \qquad (42)$$

while FP is approximately linear even farther. A comparison of FP and FLI can be made by squaring (42) to give

$$Kt^{\frac{1}{2}} = \frac{A}{B} - \frac{A^2}{4B^{3/2}} \sqrt{1 - \frac{4B}{A^2} Z} \qquad (43)$$

Expansion of the square root term in (43) the resulting equation

$$Kt = \frac{1}{A^2} Z^2 + 2 \frac{B}{A^2} Z^3 + \ldots . \qquad (44)$$

which is similar to (38). The coefficients of Z^2 and Z^3 may be equated for a small value of Z to give A = 4.23 and B = 4.00. The values of B from a $Z/t^{\frac{1}{2}}$ versus $t^{\frac{1}{2}}$ plot is 4.16 which is in close agreement. Plots of (42) could be used for diagnostic purposes by examining the ratios of A^2/B which provide a criterion of the type of curve being examined where

$$\frac{(AK^{\frac{1}{2}})^2}{BK} = \frac{I^2}{S} \qquad (45)$$

S equals the slope and I equals the intercept on the vertical axis. The ratio of A^2/B equals 4.5 to 4.7 for the Parabolic Law and 3.8 for Fick's Linear Isotherm. This difference is not large especially when the rate data are obtained from materials that only roughly approximate spheres and are composed of a range of particle sizes[21]. A better criterion is the value of B of the adsorption isotherm. Equations for spheres, cylinders and platelets in the Parabolic Law and Fick's Linear Isotherm forms are summarized in Table 5.

TABLE 5

EQUATIONS FOR FICK'S LINEAR ISOTHERM & PARABOLIC LAW

PARTICLE SHAPE	EQUATION FORM	FLI[21]	FP[23]
SPHERE	EXACT	$1-Z = \left(\frac{6}{\pi^2}\right) \sum_{n=1}^{\infty} \left(\frac{1}{2}\right) \exp-(\pi^2 n^2 K_3 t)$	$\frac{(1-Z)}{3} - \frac{(1-Z)}{2} + \frac{1}{6} = K_3 t$
	LINEAR	$Z = \left(\frac{6}{\pi^{\frac{1}{2}}}\right) (K_3 t)^{\frac{1}{2}} - 3K_3 t \qquad (Z<0.87)$	
	LIMITING FORM*	$\frac{\pi Z^2}{36} + \frac{\pi^2 Z^3}{216} = K_3 t$	$\frac{Z^2}{18} + \frac{2}{81} Z^3 = K_3 t$
CYLINDER	EXACT	$1-Z = 4 \sum_{i=1}^{\infty} \left(\frac{1}{ji^2}\right) \exp-(j^2 i\, K_2 t)$	$(1-Z)\ \ln(1-Z) + Z = 4K_2 t$
	LINEAR	$Z = \left(\frac{4}{\pi^{\frac{1}{2}}}\right) (K_2 t)^{\frac{1}{2}} - K_2 t - \left(\frac{1}{3\pi^{\frac{1}{2}}}\right) (K_2 t)$ $(Z<0.73)$	
	LIMITING FORM*	$\frac{\pi Z^2}{64} + \frac{\pi^2 Z^3}{512} = K_2 t$	$Z^2 + \frac{Z^3}{3} = 2K_2 t$

TABLE 5 (Continued)

PLATELET	EXACT	$1-Z = \left(\frac{8}{\pi^2}\right) \sum_{n=0}^{\infty} [1/(2n+1)^2] \exp -(2n+1)^2 \left(\frac{\pi^2 K_1 t}{4}\right)$	$Z^2 = 2Kt$
	LINEAR	$Z = \left(\frac{2}{\pi^{\frac{1}{2}}}\right) (K_1 t)^{\frac{1}{2}}$ (Z<0.45)	
	LIMITING FORM*	$\frac{4}{\pi} Z^2 = K_1 t$	$Z^2 = 2Kt$

* For small values of Z

Fick's Linear Isotherm : $K_1 = D/\ell^2$, $K_2 = D/a^2$, $K_3 = D/r^2$ where ℓ is half the thickness of the platelet, a is the radius of the cylinder, r is the radius of the sphere and D is the Diffusivity.**

j_1 has the following values : $j_1 = 2.405$, $j_2 = 5.520$, $j_3 = 8.654$.

Parabolic Law : $K_1 = DC_o/Q_\infty \ell^2$, $K_2 = DC_o/Q_\infty a^2$ and $K_3 = DC_o/Q_\infty r^2$ where C_o is the concentration at time = 0 and Q_∞ is the volume adsorbed at time $\to \infty$.

** If adsorption occurs, there values should be multiplied by C_o/Q_∞.

7. RESULTS

7.1 Numerical Results

The numerical results for a given value of B are printed out as concentrations at different positions within the particle with increasing time. The approach to equilibrium factor, Z, is also calculated for each time. Tables of results are found in the Appendix for the particle shapes investigated.

Tables 8 to 13 are concerned with diffusion into a sphere. In the case of the Parabolic Law and Fick's Linear isotherm, the non-dimensional time, T, is incorporated in the equations solved. For the numerical solutions, time is multiplied by (1+B) to give T. Tables 7 to 12 are shown graphically in Figure 8 as Z versus $T^{\frac{1}{2}}$. This shows that as the parameter B is increased form 0.0 for which Fick's Linear Isotherm (FLI) is the exact solution, it approaches the Parabolic Law (FP). The concentration profiles versus the distance from the center of the sphere are found in Figure 9 for different values of B. To obtain the volume adsorbed; T/a, profiles the value of B and the value of C at different positions are inserted into the Langmuir equation

$$\frac{T}{a} = \frac{BC}{1+BC} \qquad (46)$$

Figure 10 summarizes T/a versus r/R. It shows that as B increases, the adsorption rate curve becomes more rectangular, that is it approaches the Parabolic Law.

Figures 11 and 12 show the results in terms of Z versus $T^{\frac{1}{2}}$ for the cylinder and platelet cases.

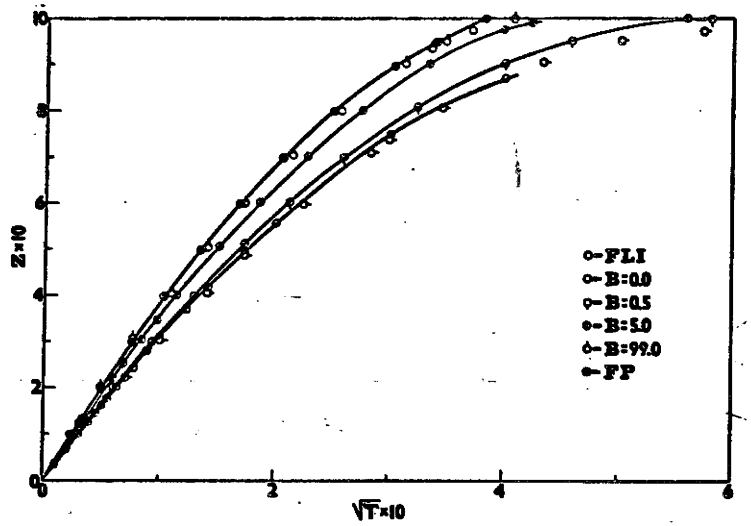

FIGURE 8
Approach to Equilibrium Factor, Z, versus Non-dimensional Time, $T^{\frac{1}{2}}$, for Diffusion into a Sphere.
- 0 : Exact Solution for FLI, (B = 0.0);
- Ø : Numerical Solution for B = 0.0;
- O : Numerical Solution for B = 0.5;
- O : Numerical Solution for B = 5.0;
- O : Numerical Solution for B = 99.0;
- O : Exact Solution for FP, (B → ∞).

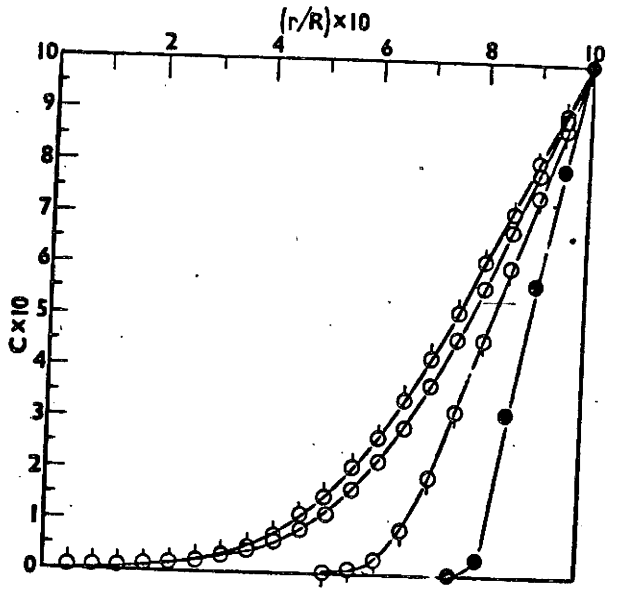

FIGURE 9
Concentration Profiles for Diffusion into a Sphere as a Function of r/R from the Numerical Solutions:
- O : B = 0.0; Z = 0.5206
- O : B = 0.5; Z = 0.506
- O : B = 5.0; Z = 0.493
- O : B = 99.0 Z = 0.4999

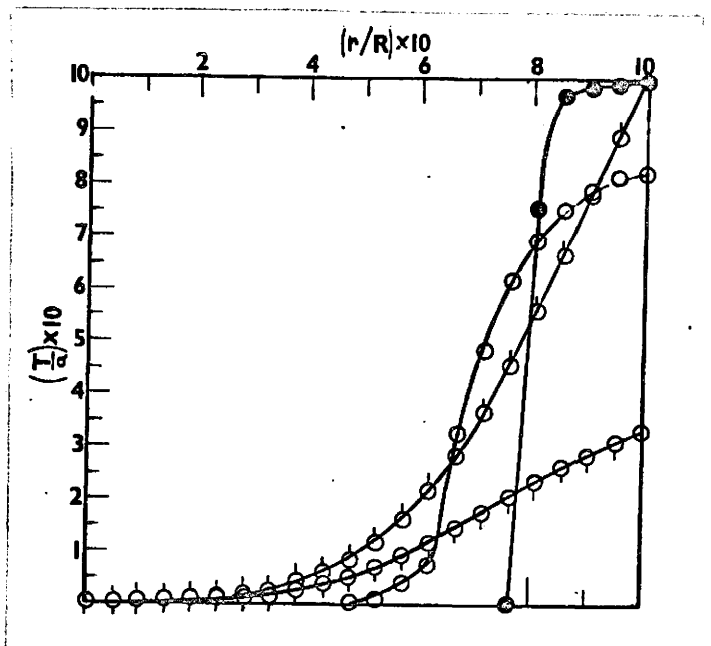

FIGURE 10:
Volume Adsorbed, T/a, Profiles for Diffusion into a Sphere as a Function of r/R from the Numerical Solutions.

♁	:	B = 0.0; Z = 0.5206
♀	:	B = 0.5; Z = 0.506
○	:	B = 5.0; Z = 0.493
●	:	B = 99.0, Z = 0.4999

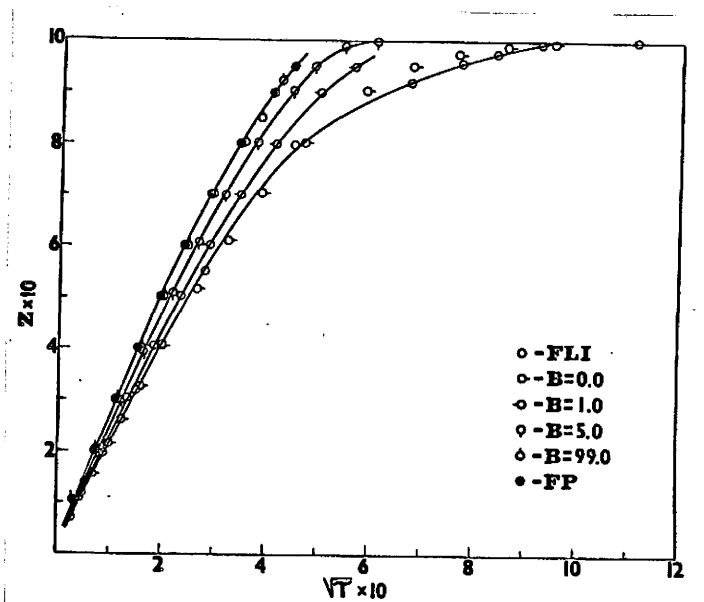

FIGURE 11:
Approach to Equilibrium Factor, Z, versus Non-dimensional time, $T^{\frac{1}{2}}$, for Diffusion into a Cylinder

- 0 : Exact Solution for FLI, (B = 0.0)
- O : Numerical Solution for B = 0.0;
- O : Numerical Solution for B = 1.0;
- O : Numerical Solution for B = 5.0;
- O : Numerical Solution for B = 99.0;
- O : Exact Solution for FP, (B → ∞).

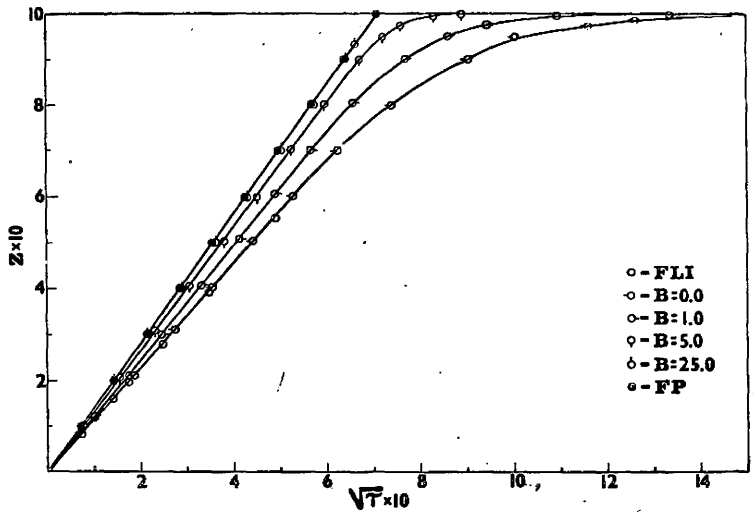

FIGURE 12:
Approach to Equilibrium Factor, Z, versus Non-dimensional time, $T^{\frac{1}{2}}$, for Diffusion into a Platelet.

O : Exact Solution for FLI, (B=0.0);
O : Numerical Solution for B = 0.0;
O : Numerical Solution for B = 1.0;
O : Numerical Solution for B = 5.0;
O : Numerical Solution for B = 25.0;
O : Exact Solution for FP, (B→∞).

7.2 EXPERIMENTAL RESULTS

Adsorption rate curves were determined at constant temperature and pressure. For Type 3A, it was found that the gases used; nitrogen, carbon dioxide, methane and ethane; there was no adsorption because the molecules were too large to enter the apertures of the crystal structure.

On Type 4A molecular sieves, the rates were found to be in the following order.

$$CO_2 > N_2 > CH_4 > C_2H_6$$

The experimental data were obtained on a volumetric adsorption apparatus (5.1) and is found in Appendix I. The rate data were plotted as the volume adsorbed, Q, versus the square root of time, $t^{\frac{1}{2}}$, and also as Z versus $t^{\frac{1}{2}}$. Figure 13 shows rate curves for nitrogen on Type 4A compressed powder at -78°C. Figures 14, 15, 16 and 17 show rate of adsorption and desorption for methane on Type 4A compressed powder at -78°, 0°, 30° and 50°C, respectively. A summary of adsorption isobars at 1.0 atm for different temperatures is shown in Figure 18. An inflection point is evident on curve 1 of Figure 14 and 18 at very small times. Figures 19, 20 and 21 show rate curves for ethane on Type 4A compressed powder at 0°, 30° and 50°C respectively. A summary of adsorption rate curves is also shown for ethane in Figure 22. In Figure 22, the inflection point is more evident for ethane at -78°C. This point occurs at all temperatures but because the adsorption is too rapid at higher temperatures, it is not noticeable. Figures 23,

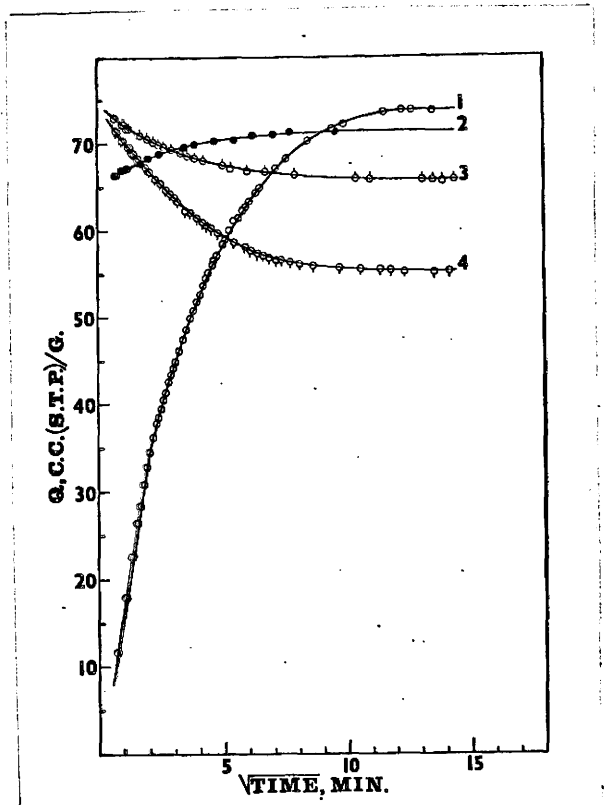

FIGURE 13:
Adsorption and Desorption Rate Curves for N_2 on Type 4A Compressed Powder at -78°C.
Curve 1 : 1.00 atm;
2 : from 0.50 to 0.75 atm;
3 : from 1.00 to 0.50 atm;
4 : from 1.00 to 0.25 atm.

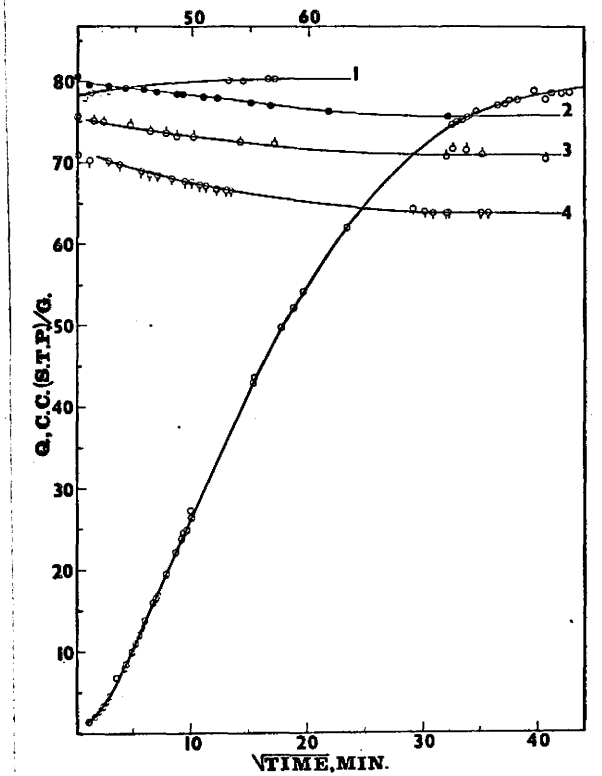

FIGURE 14:
Adsorption and Desorption Rate Curves for CH_4 on Type 4A Compressed Powder at -78°C.
Curve 1 : 1.00 atm;
2 : from 1.00 to 0.75 atm;
3 : from 0.75 to 0.50 atm;
4 : from 0.50 to 0.25 atm.

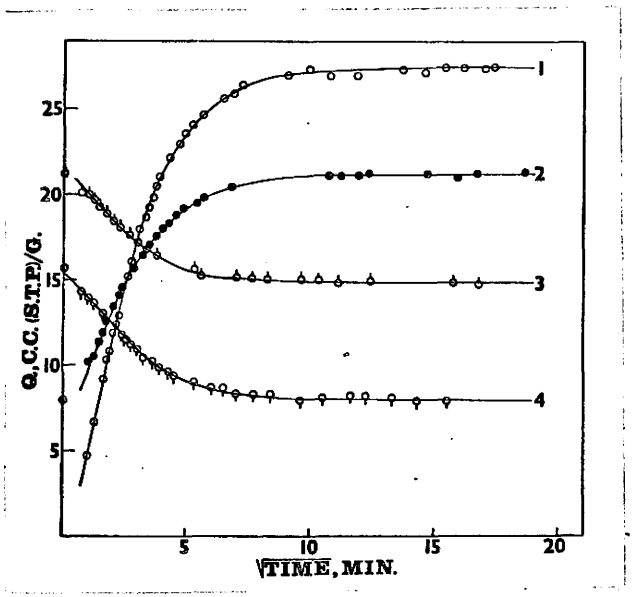

FIGURE 15:
Adsorption and Desorption Rate Curves for CH_4 on Type 4A Compressed Powder at 0°C.
Curve 1 : 1.00 atm;
2 : from 0.25 to 0.75 atm;
3 : from 0.75 to 0.50 atm;
4 : from 0.50 to 0.25 atm.

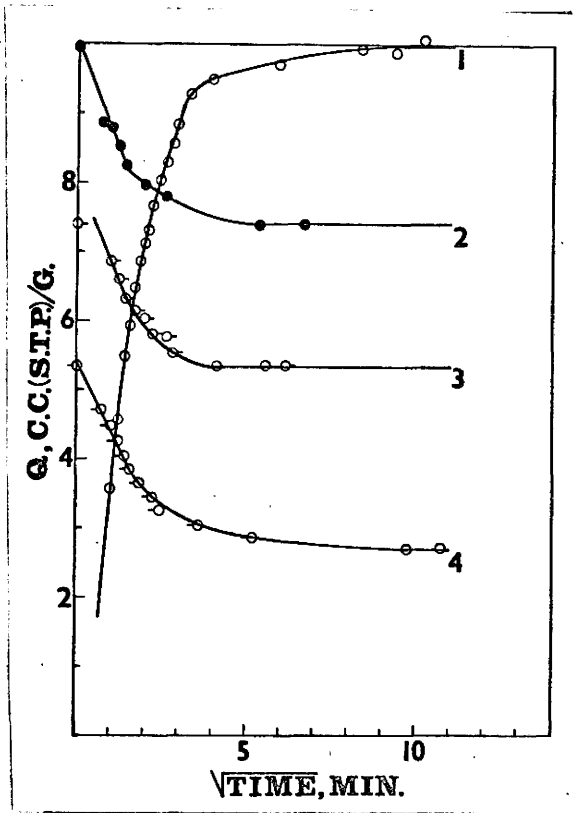

FIGURE 16:
Adsorption and Desorption Rate Curves for CH_4 on Type 4A Compressed Powder at 30°C.
Curve 1 : 1.00 atm;
2 : from 1.00 to 0.75 atm;
3 : from 0.75 to 0.50 atm;
4 : from 0.50 to 0.25 atm.

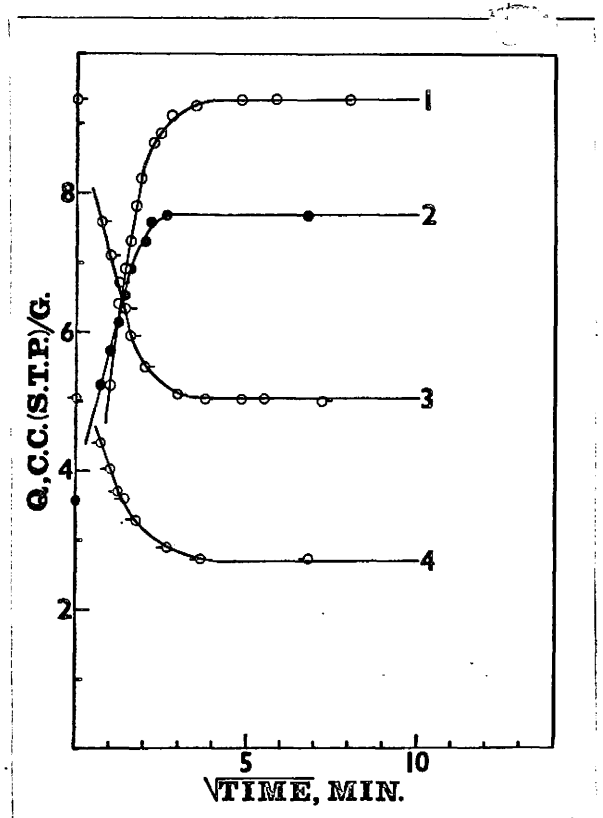

FIGURE 17:
Adsorption and Desorption Rate Curves for CH_4 on Type 4A Compressed Powder at 50°C.
Curve 1 : 1.00 atm;
2 : from 0.33 to 0.75 atm;
3 : from 1.0 to 0.50 atm;
4 : from 0.50 to 0.25 atm.

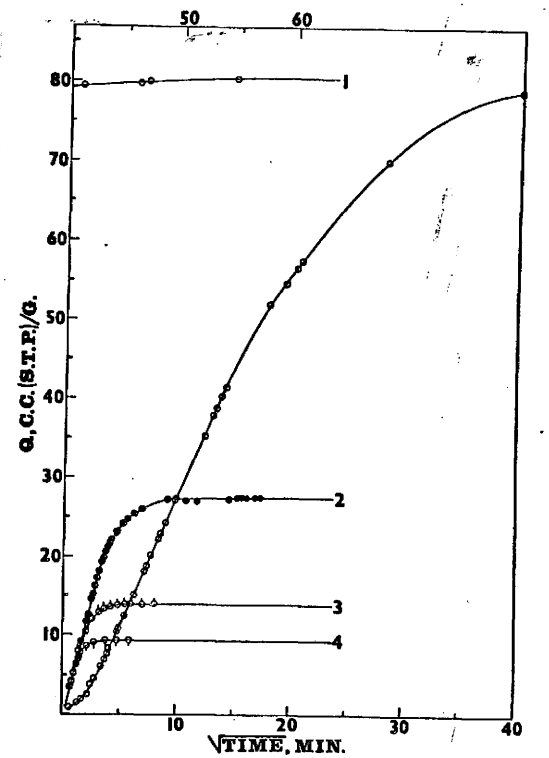

FIGURE 18:
Adsorption Rate Curves for CH_4 on Type 4A Compressed Powder at 1.00 atm.
Curve 1 : -78°C;
2 : 0°C;
3 : 30°C;
4 : 50°C.

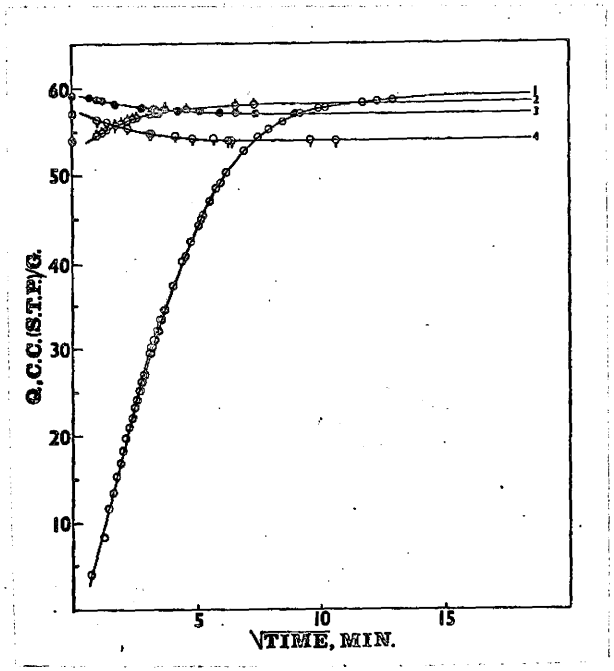

FIGURE 19:
Adsorption and Desorption Rate Curves for C_2H_6 on Type 4A Compressed Powder at 0°C
Curve 1 : 1.00 atm;
2 : from 0.25 to 0.75 atm;
3 : from 1.00 to 0.50 atm;
4 : from 0.50 to 0.25 atm.

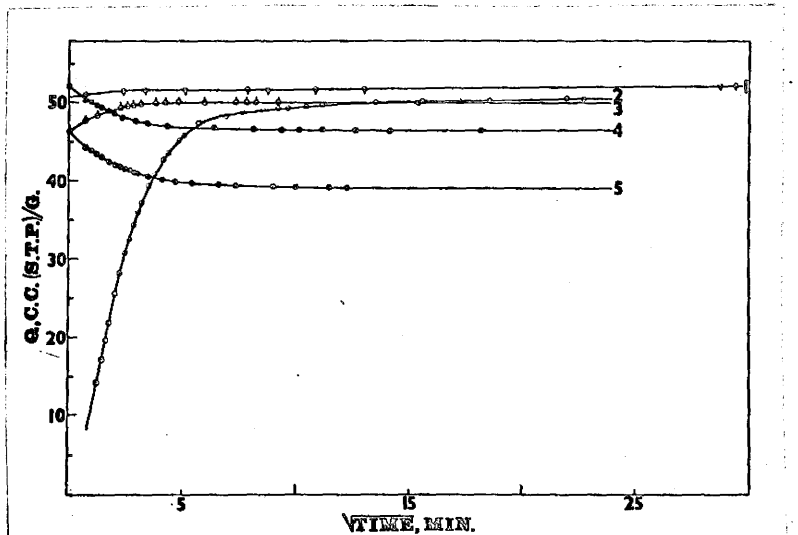

FIGURE 20:
Adsorption and Desorption Rate Curves for C_2H_6 on Type 4A Compressed Powder at 30°C.
Curve 1 : from 0.87 to 1.00 atm;
2 : 0.87 atm;
3 : from 0.50 to 0.75 atm;
4 : from 1.00 to 0.50 atm;
5 : from 0.50 to 0.25 atm.

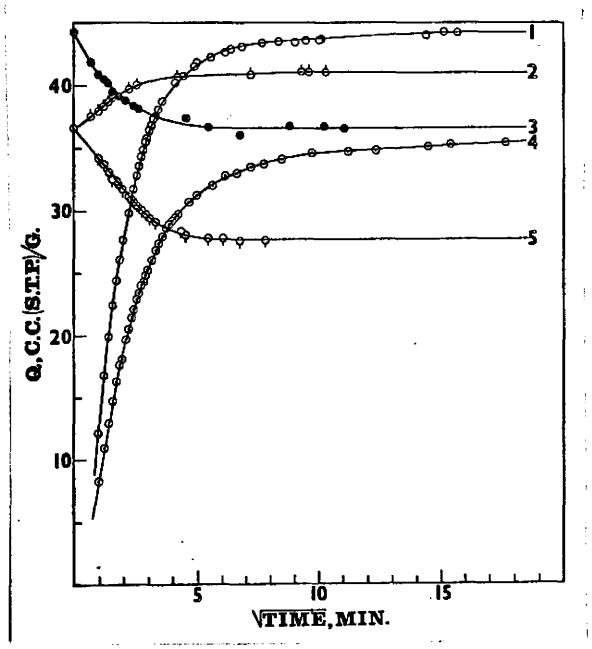

FIGURE 21:
Adsorption and Desorption Rate Curves for C_2H_6 on Type 4A Compressed Powder at 50°C.
Curve 1 : 1.00 atm;
2 : from 0.50 to 0.75 atm;
3 : from 1.00 to 0.50 atm;
4 : 0.50 atm;
5 : from 0.50 to 0.25 atm.

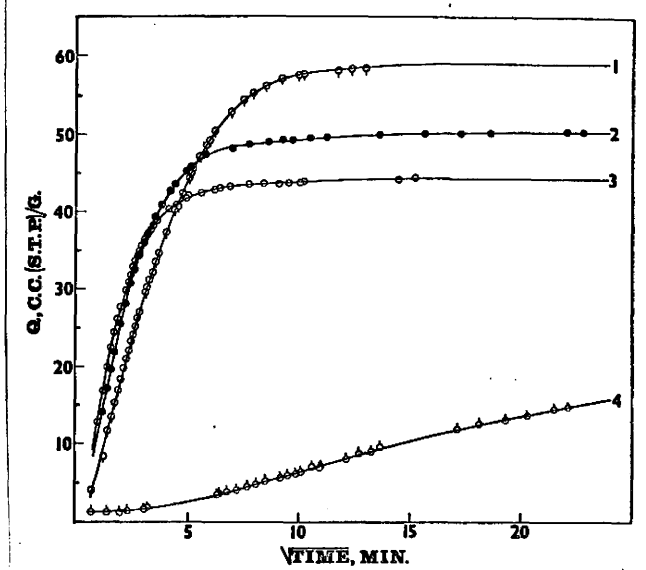

FIGURE 22:
Adsorption Isobars for C_2H_6 on Type 4A Compressed Powder.
Curve 1 : 50°C and 1.00 atm;
2 : 30°C and 0.87 atm;
3 : 0°C and 1.00 atm;
4 : -78°C and 1.00 atm.

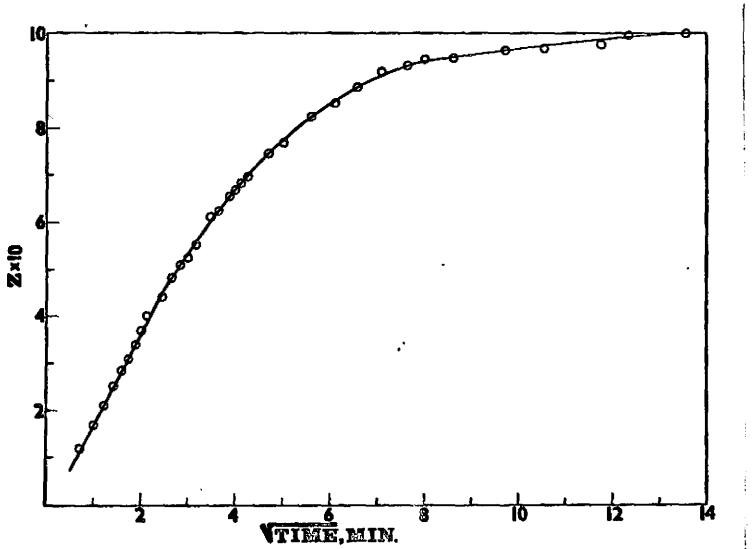

FIGURE 23:
Approach to Equilibrium Factor, Z, versus $\sqrt{\text{Time}}$ for N_2 at -78°C and 1.00 atm on Type 4A Compressed Powder.

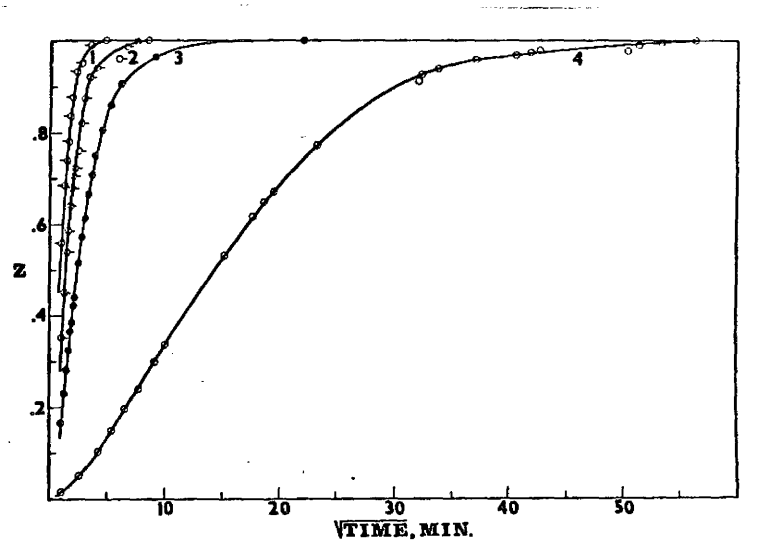

FIGURE 24:
Approach to Equilibrium Factor, Z, versus $\sqrt{\text{Time}}$ for CH_4 at 1.00 atm on Type 4A Compressed Powder.

Curve 1 : 50°C;
2 : 30°C;
3 : 0°C;
4 : -78°C.

24 and 25 show plots of Z versus $t^{\frac{1}{2}}$ from Nitrogen, Methane and Ethane respectively.

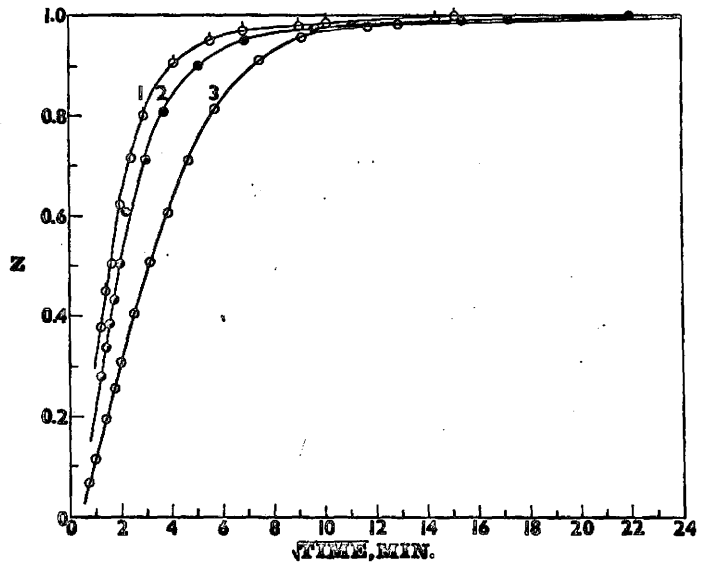

FIGURE 25:
Approach to Equilibrium Factor, Z, verus $\sqrt{\text{Time}}$ for C_2H_6 on Type 4A Compressed Powder.

Curve 1 : 50°C and 1.00 atm;
2 : 30°C and 0.87 atm;
3 : 0°C and 1.00 atm

8. EXPERIMENTAL TREATMENT

These experimental data were treated by using the Parabolic Law (PL) with time dependent surface equilibration. The diffusivity, D, is also assumed constant in this case. This point of inflection may be possibly explained by the superimposition of another time dependent term upon the process such as equilibration of the surface. The reasons for using the PL are that it is simple and that in some cases the experimentally determined isotherms were very close to being rectangular. A workable equation can be developed by making the following substitution in (26).

$$C_o' = C_o (1 - e^{-at}) \tag{47}$$

and carry out the same method of solution to give

$$\frac{-(1-Z)^{2/3}}{2} + \frac{1-Z}{3} + \frac{1}{6} = K[t - \frac{1}{a}(1 - e^{-at})] \tag{48}$$

The left handside of (48) is equated to F(Z) so that

$$F(Z) = K[t - \frac{1}{a}(1 - e^{at})]$$

F(Z) can be evaluated for any value of Z. A plot of F(Z) versus time should give a straight line where the slope equals K and the intercept equals $\frac{1}{a}$. For longer times (49) reduces to

$$F(Z) = K(t - \frac{1}{a})$$

Figure 26 is a plot of F(Z) versus time for Nitrogen adsorption on Type 4A pellets (1/16") at -78°C. Figure 27

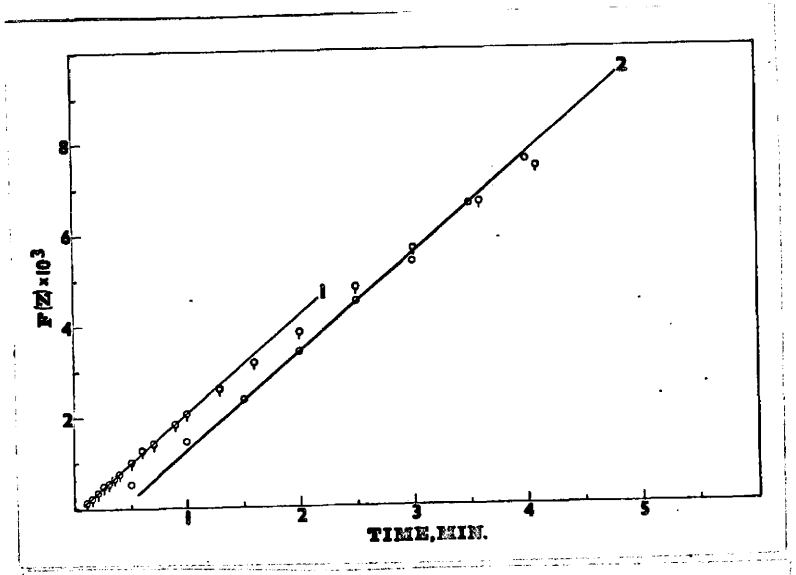

FIGURE 26:
F(Z) versus Time for Nitrogen Adsorption on Type 4A Pellets (1/16") at -78°C and 1.00 atm.
1 : 10x Scale as shown;
2 : Scale as shown.

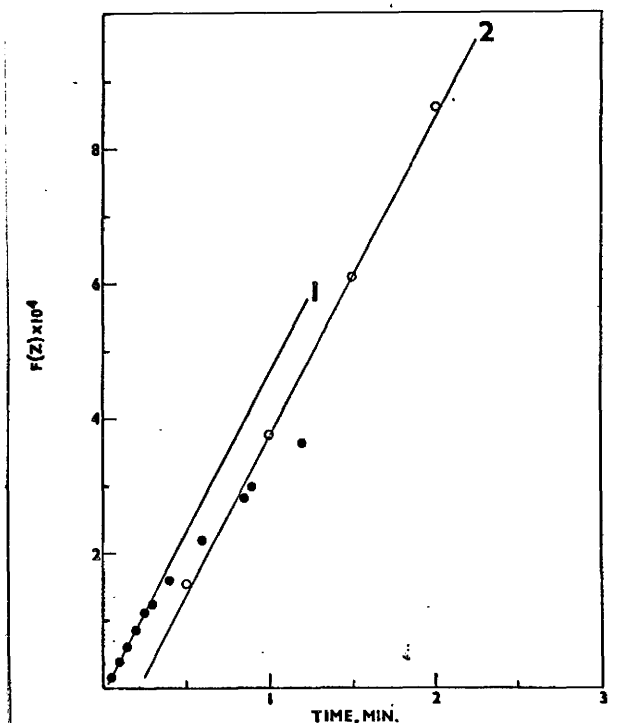

FIGURE 27:
F(Z) versus Time for Nitrogen Adsorption on Type 4A Compressed Powder at -78°C and 1.0 atm.
1 : 10X Scale as shown
2 : Scale as shown.

is for Nitrogen on 4A Compressed Powder at -78°C. Figures 28 to 32 show the results for Methane on Type 4A molecular sieve at -78°, 0°, 30° and 50°C. For Ethane similar plots are obtained as seen in Figures 33 to 35. In Figure 35 there are two sets of plots, one at 1.0 atm and the other at 0.5 atm. This was done as a check on the results obtained and summarized in Table 6. The equation as developed fits data for $0.05 < Z < 0.95$.

The closer the experimental data are to PL, the closer to equilibrium the equation holds before breaking away. Figure 36 shows how close (49) predicts the experimental data which in this case is Methane Adsorption on Type 4A Compressed Powder at -78°C. On this plot of Z versus $\sqrt{\text{Time}}$, the equation holds well until $Z > 0.95$.

From the slope, K, obtained from the F(Z) versus Time plots we can evaluate D/R^2 since $K = (DC_o/R^2Q_\infty)$ and we have values for C_o and Q_∞. $C_o = 273\ P/T$ where P is in atm and T is in degrees Kelvin. The diffusivity can be calculated since a value for R was obtained from electron microscope examination. A value for the Diffusivity based on the porosity of the particle, D_e can be calculated by dividing D by $\theta/\sqrt{2}$ where θ is the proosity [8] and $\sqrt{2}$ is the Deviousness Factor [25]. The above values are summarized in Table 6. For purposes of comparison, Diffusivities were calculated with the equation for Knudsen Diffusion [24].

$$D_K = 9.7 \times 10^3 r \sqrt{\frac{T}{M}} \quad \frac{cm^2}{sec} \qquad (51)$$

where T is in °K, M is the molecular weight and r is the radius of the pores. These values were found to be in the order of 10^9 larger than those calculated from F(Z) versus Time plots.

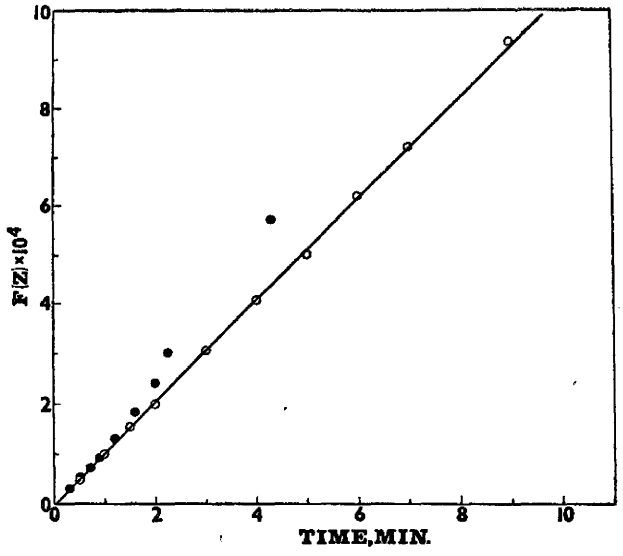

FIGURE 28:
F(Z) versus Time for Methane Adsorption on Type 4A Pellets (1/16") at -78°C and 1.0 atm.
0 : Scale as shown
● : 10X Scale as shown.

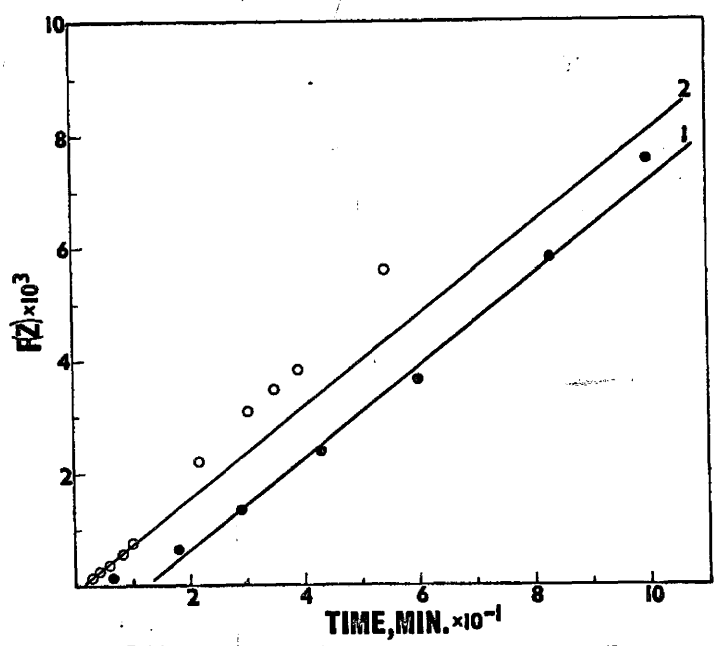

FIGURE 29:
F(Z) versus Time for Methane Adsorption on Type 4A Compressed Powder at -78°C and 1.0 atm.
1 : Scale as shown
2 : 10XF(Z) scale and 10X Time Scale as shown.

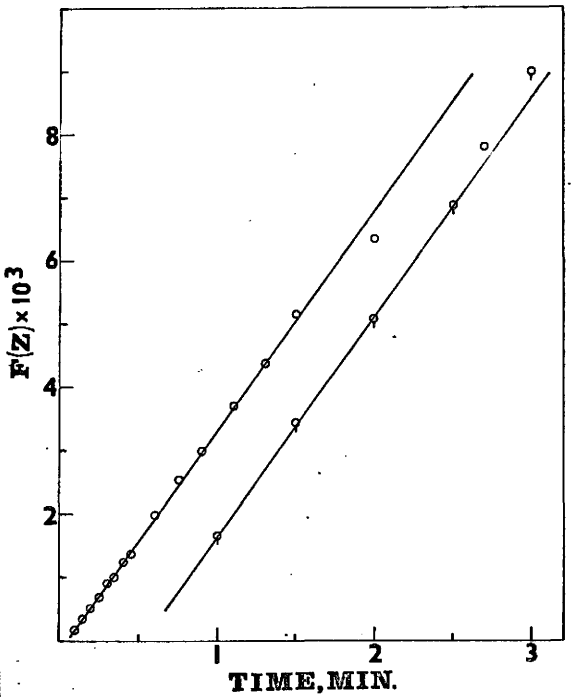

FIGURE 30:
$\overline{F(Z)}$ versus Time for Methane Adsorption on Type 4A Compressed Powder at 0°C and 1.0 atm.
Q : Scale as shown
O : 10X Scale as shown.

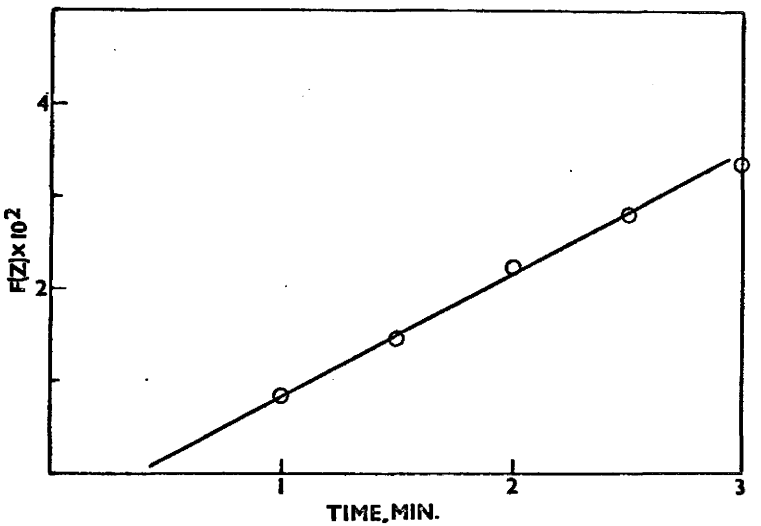

FIGURE 31:
$\overline{F(Z)}$ versus Time for Methane Adsorption on Type 4A Compressed Powder at 30°C and 1.0 atm.

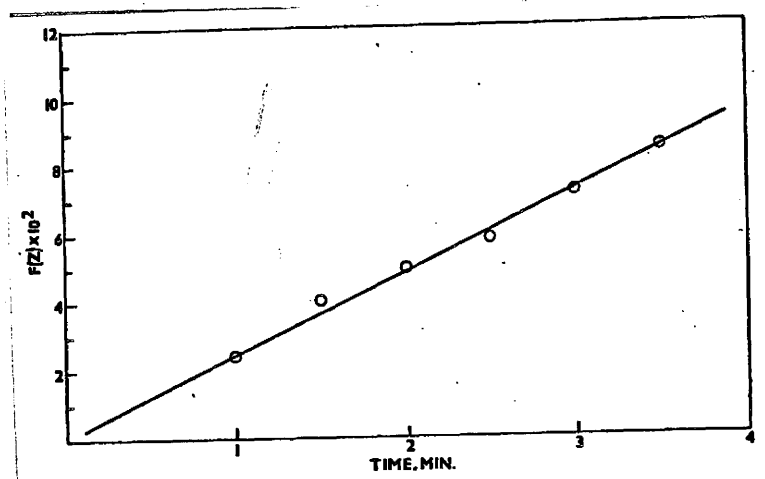

FIGURE 32:
F(Z) versus Time for Methane Adsorption on Type 4A Compressed Powder at 50°C and 1.0 atm.

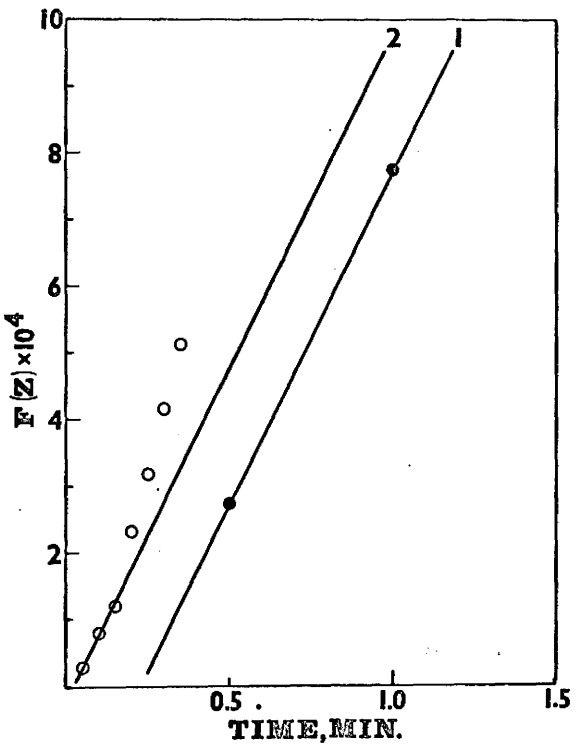

FIGURE 33:
F(Z) versus Time for Ethane Adsorption on Type 4A Compressed Powder at 0°C and 1.0 atm.
1 : Scale as shown
2 : 10X Scale as shown.

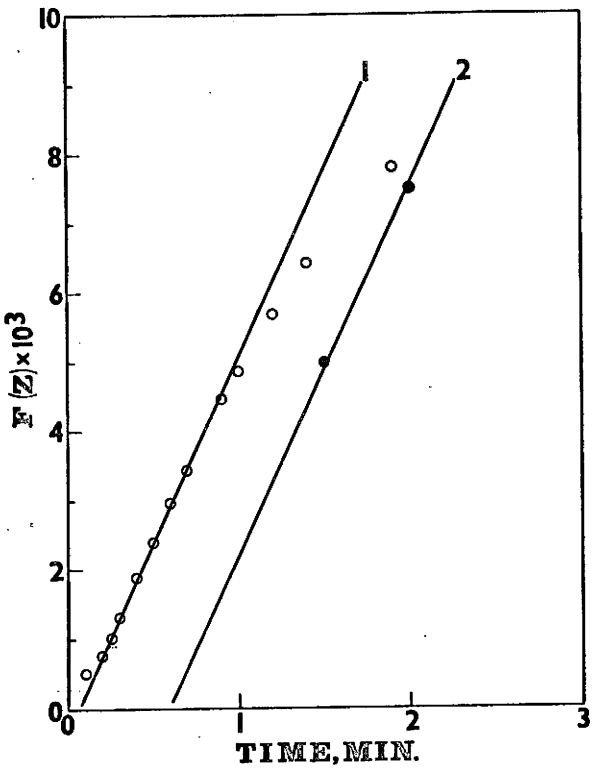

FIGURE 34:
F(Z) versus Time for Ethane Adsorption on Type 4A Compressed Powder at 30°C and 0.87 atm.
1 : 10X Scale as shown
2 : Scale as shown.

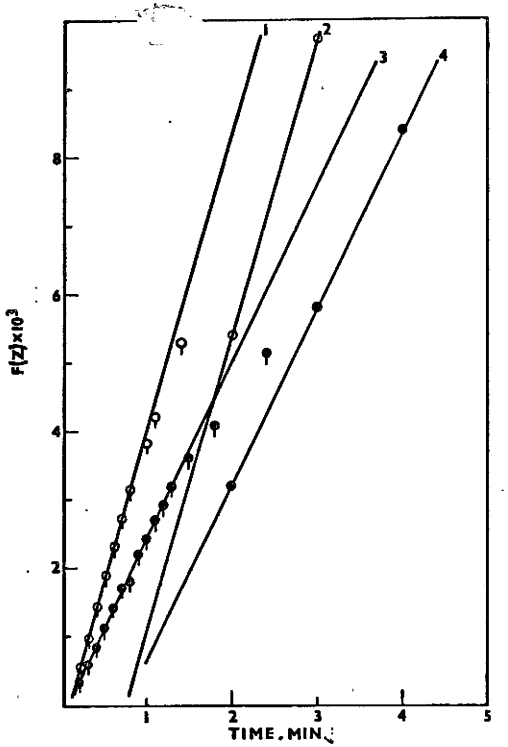

FIGURE 35:
F(Z) versus Time for Ethane Adsorption on Type 4A Compressed Powder at 50°C.
1 : 10X Scale as shown and 1.0 atm.;
2 : Scale as shown and 1.0 atm.;
3 : 10X Scale as shown and 0.50 atm.;
4 : Scale as shown and 0.50 atm.

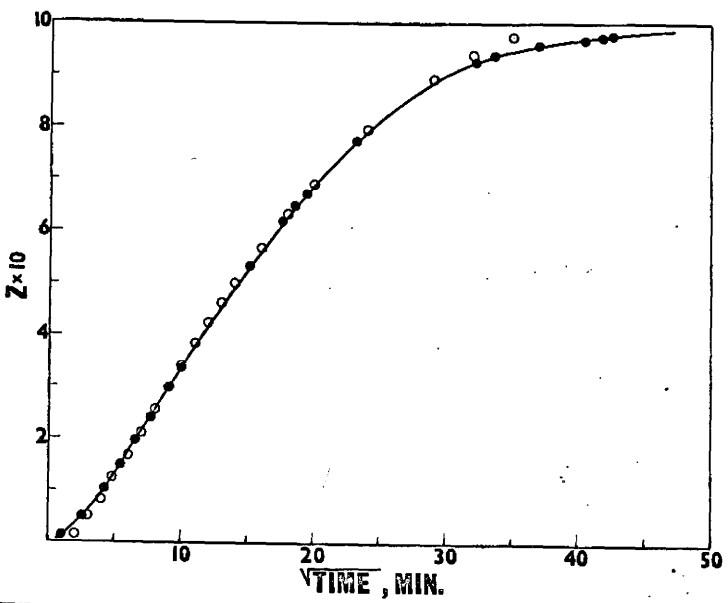

FIGURE 36
Comparison of $F(Z) = K[t - \frac{1}{a}(1-e^{-at})]$ and experimental data for methane at -78°C in terms of Z versus $\sqrt{Time}$.

O : Methane at -78°C;

O : $F(Z) = K[t - \frac{1}{a}(1-e^{-at})]$

TABLE 6

Values of D/R^2 and, D_θ and 1/a obtained from F(Z) versus Time plots[1].

Sample[2]	Gas	Temp, °C	1/a	K x 10^3	(D/R^2) x 10^3	D_θ x 10^{13}
Pellet	N_2	-78	0.42	2.15	2.18	12.06
Powder	"	-78	0.21	30.35	5.50	4.73
Pellet	CH_4	-78	0.07	0.10	0.13	0.71
Powder	"	-78	12.10	0.82	0.10	0.57
"	"	0[3]	0.53	3.47	2.13	11.76
"	"	30[3]	0.37	13.26	4.73	26.12
"	"	50[3]	0.00	24.00	5.89	32.49
Powder	C_2H_6	0	0.23	1.07	1.41	7.73
"	"	30[1]	0.59	5.42	7.72	42.60
"	"	50	0.38	8.68	10.03	55.36
"	"	50[1]	0.37	5.16	9.88	54.57

1. All samples were at 1.00 atm except for ethane at 30° and 50°C which were 0.87 and 0.50 atm respectively.

2. Type 4A Compressed Powder or Type 4A Compressed Pellet (1/16").

3. These runs had low values of B (B<1), therefore PL is strictly not applicable. In this case FLI would be more appropriate.

Activation energies can be determined graphically from plots of $\ell n \frac{D}{R^2}$ versus $\frac{1}{T}$, where T is in degrees Kelvin. Figure 37 is such a plot of $\ell n \frac{D}{R^2}$ versus $\frac{1}{T}$ and the slopes give activation energies of 4.1 Kcal/gmole for methane and 6.0 Kcal/gmole for ethane. Heats of adsorption can be obtained from plots of ℓn p versus $\frac{1}{T}$ where p is the pressure in atm at constant adsorption. These were found to be 7.2 Kcal/gmole for methane and 8.3 Kcal/gmole for ethane.

The constants a and b in the Langmuir equation can be determined from plots of $\ell n\ Q_\infty$ versus $\ell n\ C_o$. Figures 38 to 41 show these plots for nitrogen, carbon dioxide, methane and ethane. The constant b is obtained from a ratio of Q_∞ at two different pressures, i.e. 0.25 and 1.0 atm., with the use of the Langmuir equation. The value of b can then be substituted back into the Langmuir equation to give a. Table 7 summarizes these constants. Some of the B values were not as large as expected ($B < 1.0$) since $bC_o = B$. Therefore some of the adsorption rate curves were more similar to FLI than to FP.

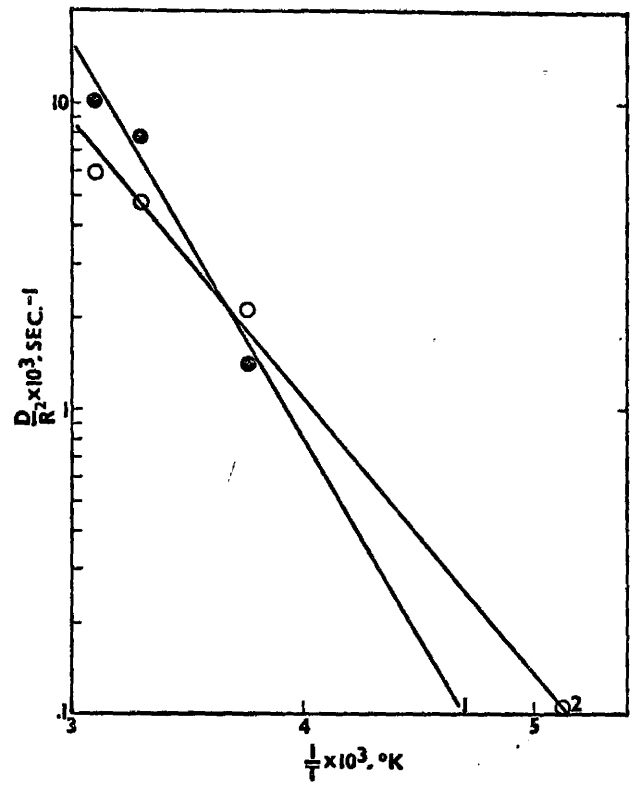

FIGURE 37:
Ln D/R^2 versus Reciprocal Temperature.
1 : Ethane
2 : Methane.

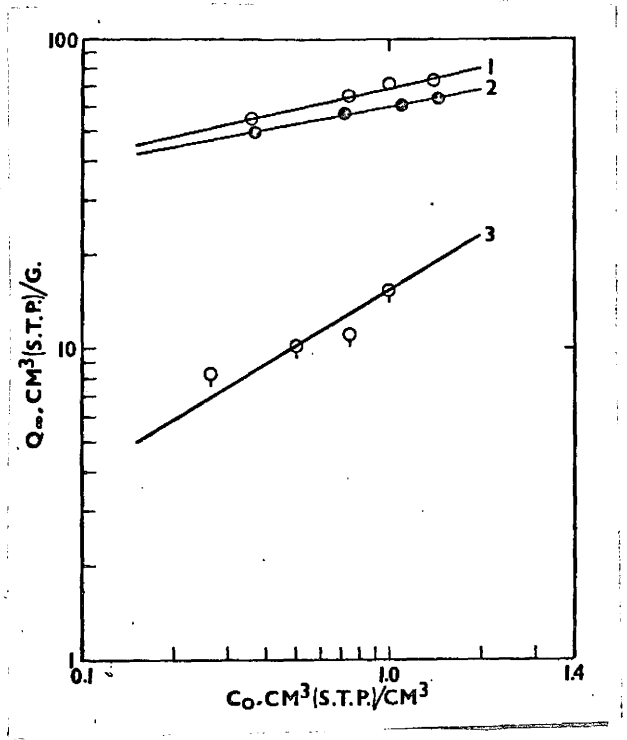

FIGURE 38
Ln Q_∞ versus ℓnC_o for Nitrogen Adsorption

1 : Type 4A Compressed Powder at -78°C;
2 : Type 4A Platelets (1/16") at -78°C;
3 : Type 4A Compressed Powder at 0°C.

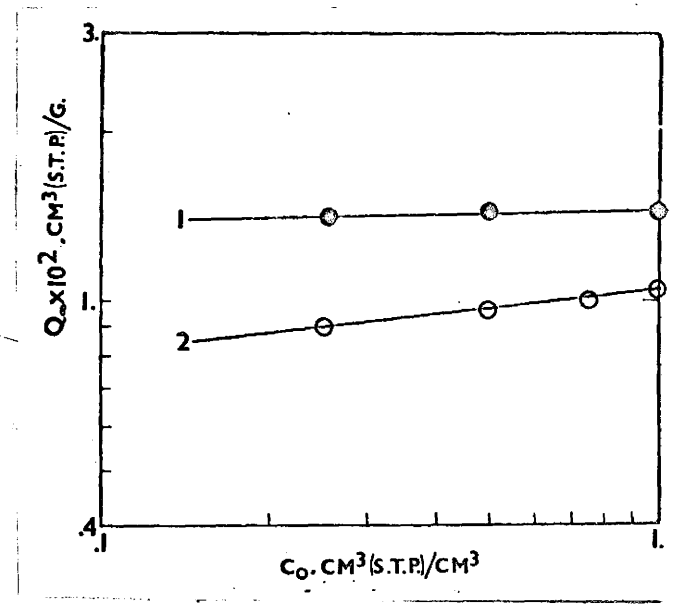

FIGURE 39
Ln Q_∞ versus ℓnC_o for Carbon Dioxide Adsorption on Type 4A Compressed Powder.

1 : -78°C;
2 : 0°C.

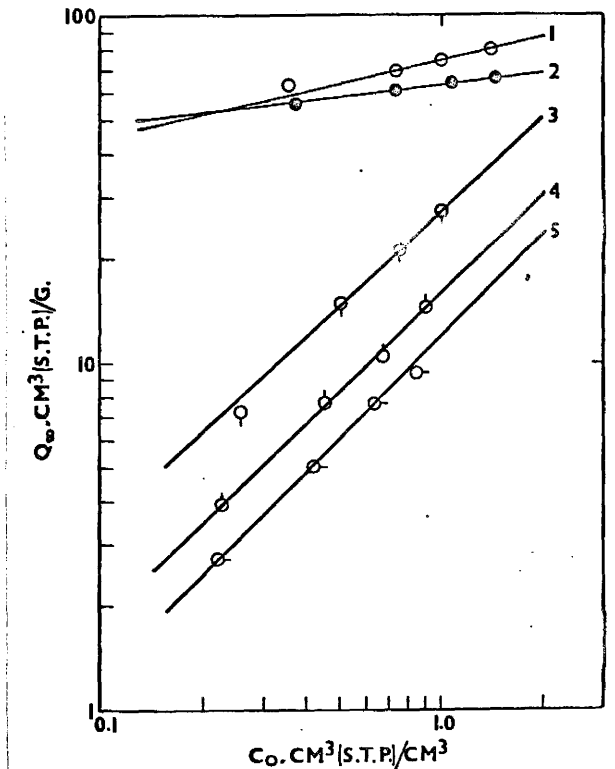

FIGURE 40:
Ln Q_∞ versus ℓnC_o for Methane Adsorption on Type 4A Compressed Powder

1 * : -78°C;
2 : -78°C;
3 : 0°C;
4 : 30°C;
5 : 50°C.

* Type 4A Pellet

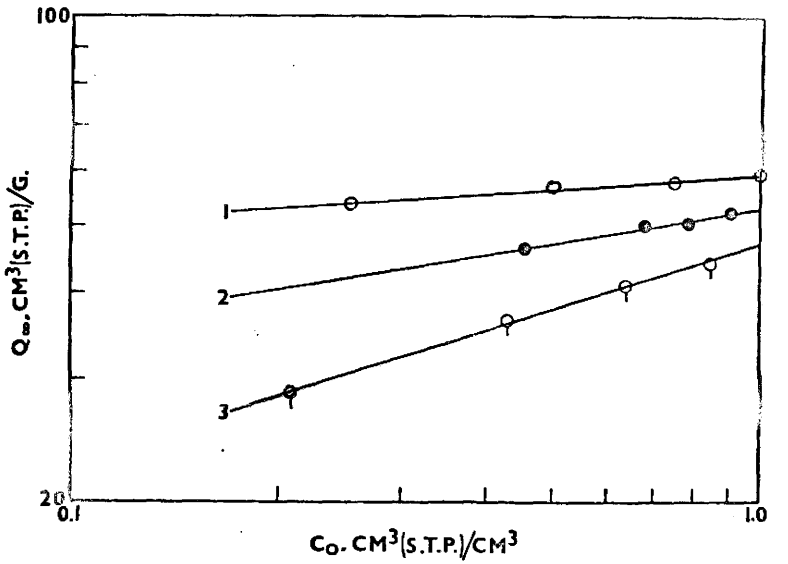

FIGURE 41:
Ln Q_∞ versus ℓnC_o for Ethane Adsorption on Type 4A Compressed Powder

1 : 0°C;
2 : 30°C;
3 : 50°C.

TABLE 7

Values of the Langmuir constants a and b obtained from plots of ℓnQ_∞ versus C_o.

SAMPLE[1]	Gas	Temp, °C.	b[2]	a
Powder	N_2	-78	10.6	75.5
"	"	0	1.4	27.0
Pellet	"	-78	9.4	66.4
Powder	CO_2	-78	103.3	142.0
"	"	0	16.6	110.2
Powder	CH_4	-78	7.3	85.4
"	"	0	0.2	184.9
"	"	30	0.1	188.8
"	"	50	0.04	299.0
Pellet	"	-78	16.9	57.2
Powder	C_2H_6	0	37.4	75.1
"	"	30	10.3	58.5
"	"	50	4.5	57.7

1. Type 4A Compressed Powder or Type 4A Pellet (1/16")

2. Note $bC_o = B$

9. CONCLUSIONS AND RECOMMENDATIONS

9.1 Conclusions

(a) Numerical solutions are given for adsorption according to the Langmuir isotherm for diffusion according to Fick's law. These computed curves shift from Fick's Linear Isotherm (FLI) to theParabolic Law (FP) as the parameter B increases. For theinitial part of the rate curve, the change is small, therefore calculated values of D/R^2 for a given rate curve for FLI are 50% higher than for FP.

(b) The rates of adsorption and desorption were found to be in the following order:

$$CO_2 > N_2 > CH_4 > C_2H_6$$

This suggests behavior according to size and shape of the molecule as the higher activation energy of ethane than for methane, 6.3 versus 4.1 Kcal/mole also suggests more deformation of the ethane molecule in order to enter the zeolite than for methane.

(c) Also the time parameter contains C_o/Q_∞ to give $(C_o\ D/Q_\infty R^2)t$ which has not been included by previous workers. This gives a more correct diffusivity term since the slope of the F(Z) versus Time is used to determine diffusivities and this slope, K, equals $(C_o\ D/Q_\infty R^2)$.

(d) Neglecting the adsorption term in D/aR^2 to give D/R^2 also gives an erroneous diffusivity value.

(e) A point of inflection occurs initially with the experimental data when plotted as the volume adsorbed versus $\sqrt{\text{Time}}$.

9.2 RECOMMENDATIONS

It is recommended that further work consist of the following:

(a) Investigation of the cause of the point of inflection in the initial portion of the experiment, i.e. whether by surface equilibration or not of the Type 4A zeolite.

(b) Determination of a complete adsorption-desorption cycle of C_2H_6 at -78°C on Type 4A zeolite.

(c) Determination of a complete adsorption-desorption cycle for N_2 at - 195°C on Type 4A zeolites.

(d) Determination of rate curves at higher temperatures (>50°C) and at intermediate temperatures between - 195° and -78°C and also between -78° and 0°C with the different gases already used on the Type 4A zeolite.

(e) Investigation of adsorption on Type 5A zeolite with larger gas molecules than used in this work.

BIBLIOGRAPHY

1. Brunauer, S.,
"The Adsorption of Gases and Vapors",
Vol.1, Chapter 1, Princeton University Press (1943).

2. Hersh, C.K.,
"Molecular Sieves",
Chapter 2, Reinhold Publishing Corp., New York (1961).

3. Barrer, R.M.
"Diffusion in and through Solids",
Cambridge at the University Press, (1951).

4. Crank, J.,
"The Mathematics of Diffusion",
Oxford at the Claredon Press, (1956).

5. Emmett, P.H., and T.W. Dewitt,
J.Am.Chem.Soc., 65, 1253 (1943).

6. Ross, S., and J.P. Olivier,
"On Physical Adsorption",
2, 31, Interscience Publishers, New York, (1964).

7. Barrer, R.M.,
Chem.Soc.Ann.Reports, 41, 31 (1944).

8. Buck, D.W.,
J.Chem.Education, 41, 678 (1964).

9. Barrer, R.M.,
Proc.Roy.Soc., London, A.167, 393 (1938).

10. Barrer, R.M.,
Trans.Faraday Soc., 40, 374 (1944).

11. Barrer, R.M. and D.A. Ibbitson,
Trans.Faraday Soc., 40, 195 (1944).

12. Lamb, A.B. and J.C. Woodhouse,
J.Am.Chem.Soc., 58, 2637, (1936).

13. Barrer, R.M., and D, Riley,
J.Chem.Soc., 133 (1948).

14. Nelson, E.T. and P.L. Walker,
J.Appl.Chem. 11, 358 (1949).

15. Barrer, R.M.,
Trans.Faraday Soc., 45, 358 (1949).

16. Barrer, R.M.,
J.Chem.Soc., 2158 (1948).

17. Barrer, R.M.,
Discussions Faraday Soc., 40, 206 (1944).

18. Breck, D.W., W.G. Eversole, and R.M. Milton,
J.Am.Chem.Soc., 78, 2338 (1956).

19. Linde Molecular Sieves : Adsorption Data Sheets
as supplied by Linde Division of Union Carbide
Corporation, U.S.A.

20. Hayward, D.O., and B.M.W. Trapnell,
"Chemisorption",
2nd Edition, Butterworths & Co. Ltd., Linden, p.161 (1964).

21. Anderson, R.B. et. al.
"Linear Solutions of Fick's Law",
I&EC Process Design and Development, 4, 167 (April, 1965).

22. Jenson, V.G., and G.V. Jeffreys,
"Mathematical Methods in Chemical Engineering",
Academic Press, London and New York, 9, 307 (1963)

23. Weisz, P.B. and R.D. Goodwin,
J. Catalysis, 2, 397 (1963).

24. Wheeler, A.,
"Advances in Catalysis", Vol. III,
Edited by W.G. Frankenburg et. al. Academic Press,
New York, N.Y. 257 (1951).

25. Wheeler, G,
"Catalysis : Fundamental Principles"
Vol.II, Edited by P.H. Emett, Reinhold Publishing Corp.,
New York, 127 (1955).

APPENDIX I

NUMERICAL AND EXPERIMENTAL DATA

TABLE 8.

SOLUTION OF FICK'S LINEAR ISOTHERM FOR DIFFUSION INTO A SPHERE (B = 0.0)

$T \times 10^3$	Z	$T \times 10^3$	Z	$T \times 10^3$	Z
0.1	0.034	3.0	0.176	20.0	0.419
0.4	0.067	4.0	0.202	30.0	0.496
0.9	0.099	6.0	0.244	40.0	0.557
1.5	0.127	8.0	0.279	90.0	0.746
2.0	0.145	10.0	0.309	160.0	0.874
2.5	0.162	15.0	0.370		

TABLE 9

SOLUTION OF THE PARABOLIC LAW FOR DIFFUSION INTO A SPHERE ($B \to \infty$)

$T \times 10^3$	Z	$T \times 10^3$	Z	$T \times 10^3$	Z
0.6	0.10	18.3	0.50	92.3	0.90
2.4	0.20	28.6	0.60	115.5	0.95
5.8	0.30	42.6	0.70	146.8	0.99
11.0	0.40	62.3	0.80		

TABLE 10

NUMERICAL SOLUTION FOR DIFFUSION INTO A SPHERE WITH B = 0.0

$T \times 10^3$	Z	$T \times 10^3$	Z	$T \times 10^3$	Z
5.0	0.224	50.0	0.599	255.0	0.950
10.0	0.305	80.0	0.711	330.0	0.976
20.0	0.412	90.0	0.739	420.0	0.990
30.0	0.489	120.0	0.808	490.0	0.995
		190.0	0.904	725.0	1.000

TABLE 11

NUMERICAL SOLUTION FOR DIFFUSION INTO A SPHERE WITH B = 0.5

$T \times 10^3$	Z	$T \times 10^3$	Z	$T \times 10^3$	Z
0.6	0.101	30.0	0.513	157.0	0.904
3.6	0.202	45.0	0.603	210.0	0.953
8.7	0.300	67.5	0.702	630.0	1.000
16.7	0.400	105.0	0.812		

TABLE 12

NUMERICAL SOLUTION FOR DIFFUSION INTO A SPHERE WITH B = 5.0

$T \times 10^3$	Z	$T \times 10^3$	Z	$T \times 10^3$	Z
1.2	0.133	13.2	0.401	111.6	0.902
3.6	0.223	22.8	0.507	159.6	0.976
4.8	0.253	34.8	0.603	178.8	0.990
7.2	0.305	51.6	0.702	312.0	1.000
9.6	0.348	75.6	0.802		

TABLE 13

NUMERICAL SOLUTION FOR DIFFUSION INTO A SPHERE WITH B = 99.0

$T \times 10^3$	Z	$T \times 10^3$	Z	$T \times 10^3$	Z
1.0	0.125	30.0	0.602	121.0	0.950
2.0	0.203	46.0	0.705	138.0	0.975
6.0	0.308	66.0	0.801	167.0	1.000
12.0	0.404	98.0	0.902		
20.0	0.505	113.0	0.936		

TABLE 14

CONCENTRATIONS AND VOLUME ADSORBED AS A FUNCTION OF THE DISTANCE FROM THE CENTER OF A SPHERE AT B = 0.0, Z = 0.5206 and T = 0.035

r/R	C	$\frac{T}{a} \times 10^3$
0.048	0.006	6.00
0.095	0.006	6.00
0.143	0.007	7.00
0.191	0.010	10.00
0.238	0.014	14.00
0.286	0.020	20.00
0.333	0.029	29.00
0.381	0.042	42.00
0.424	0.060	60.00
0.476	0.086	86.00
0.524	0.119	119.00
0.571	0.163	163.00
0.619	0.219	219.00
0.667	0.287	287.00
0.714	0.368	368.00
0.762	0.460	460.00
0.810	0.562	562.00
0.857	0.671	671.00
0.905	0.784	784.00
0.952	0.895	895.00
1.000	1.000	1000.00

TABLE 15

CONCENTRATION AND VOLUME ADSORBED AS A FUNCTION OF DISTANCE FROM THE CENTER OF A SPHERE AT B = 0.5, Z = 0.506 and T = 0.06

r/R	C	$\frac{T}{a} \times 10^3$
0.048	0.007	3.49
0.095	0.007	3.49
0.143	0.008	4.00
0.191	0.011	5.46
0.238	0.017	8.43
0.285	0.025	12.35
0.333	0.037	18.16
0.381	0.054	26.29
0.424	0.078	37.54
0.476	0.110	52.13
0.524	0.152	70.63
0.571	0.205	92.97
0.619	0.268	118.16
0.667	0.342	146.02
0.714	0.425	175.25
0.762	0.515	204.77
0.810	0.611	234.00
0.857	0.709	264.43
0.905	0.808	287.74
0.952	0.906	311.76
1.000	1.000	333.33

TABLE 16

CONCENTRATION AND VOLUME ADSORBED AS A FUNCTION OF DISTANCE FROM THE CENTER OF A SPHERE AT B = 5.0, Z = 0.493 & T=0.045

r/R	C	$\frac{T}{a} \times 10^3$
0.048	0.000	0.000
0.095	0.000	0.000
0.143	0.000	0.00
0.191	0.000	0.00
0.238	0.000	0.00
0.286	0.000	0.00
0.333	0.000	0.00
0.381	0.000	0.00
0.424	0.000	0.00
0.476	0.000	0.00
0.524	0.002	9.90
0.571	0.008	38.50
0.619	0.029	126.60
0.667	0.087	326.90
0.714	0.189	485.90
0.762	0.319	614.40
0.810	0.459	695.00
0.857	0.600	750.00
0.905	0.739	787.00
0.952	0.872	813.40
1.000	1.000	833.30

TABLE 17

CONCENTRATION AND VOLUME ADSORBED AS A FUNCTION OF DISTANCE FROM THE CENTER OF A SPHERE AT B = 99.0, Z = 0.4999 and T = 0.019

r/R	C	$\frac{I}{a} \times 10^3$
0.048	0.000	0.00
0.095	0.000	0.00
0.143	0.000	0.00
0.191	0.000	0.00
0.238	0.000	0.00
0.286	0.000	0.00
0.333	0.000	0.00
0.381	0.000	0.00
0.424	0.000	0.00
0.476	0.000	0.00
0.524	0.000	0.00
0.571	0.000	0.00
0.619	0.000	0.00
0.667	0.000	0.00
0.714	0.000	0.00
0.762	0.000	0.00
0.810	0.031	754.00
0.857	0.314	969.00
0.905	0.568	983.00
0.952	0.795	988.00
1.000	1.000	990.00

TABLE 18

SOLUTION OF FICK'S LINEAR ISOTHERM FOR DIFFUSION INTO A CYLINDER (B = 0.0).

$T \times 10^3$	Z	$T \times 10^3$	Z	$T \times 10^3$	Z
0.90	0.067	40.00	0.407	500.00	0.919
2.50	0.110	78.40	0.550	600.00	0.956
8.10	0.195	90.00	0.583	700.00	0.975
22.50	0.316	202.50	0.797	900.00	0.995

CORRECTION

RATES OF DIFFUSION - CONTROLLED ADSORPTION PROCESSES

G. R. Stifel, M.Eng. THESIS, October 1966.

Table 19, Page 89 should read as follows:

Table 19

Solution of the Parabolic Law for Diffusion into a Cylinder

($B \to \infty$)

Z	$\gamma \times 10^3$	$\gamma^{\frac{1}{2}}$	Z	$\gamma \times 10^3$	$\gamma^{\frac{1}{2}}$
0.1	1.2850	0.03585	0.6	58.370	0.24160
.2	5.3800	.07335	.7	84.700	.29100
.3	12.5775	.11215	.8	119.530	.34570
.4	23.3800	.15290	.9	167.435	.40915
.5	38.3500	.19580	.95	187.555	.43305

TABLE 20

NUMERICAL SOLUTION FOR DIFFUSION INTO A CYLINDER WITH B = 0.0

$T \times 10^3$	Z	$T \times 10^3$	Z	$T \times 10^3$	Z
5.00	0.155	70.00	0.515	460.00	0.951
10.00	0.213	105.00	0.611	585.00	0.975
15.00	0.258	150.00	0.703	740.00	0.990
25.00	0.326	220.00	0.802	855.00	0.995
40.00	0.403	345.00	0.904	1255.00	1.000

TABLE 21

NUMERICAL SOLUTION FOR DIFFUSION INTO A CYLINDER WITH B = 1.0

$T \times 10^3$	Z	$T \times 10^3$	Z	$T \times 10^3$	Z
2.00	0.109	55.00	0.502	251.00	0.900
8.00	0.207	84.00	0.602	320.00	0.950
18.00	0.303	122.00	0.701		
34.00	0.405	173.00	0.800		

TABLE 22

NUMERICAL SOLUTION FOR DIFFUSION INTO A CYLINDER WITH B = 5.0

$T \times 10^3$	Z	$T \times 10^3$	Z	$T \times 10^3$	Z
3.00	0.140	48.00	0.510	201.00	0.904
6.00	0.194	72.00	0.608	237.00	0.951
15.00	0.300	102.00	0.702	297.00	0.990
27.00	0.394	144.00	0.803	369.00	0.999

TABLE 23

NUMERICAL SOLUTION FOR DIFFUSION INTO A CYLINDER WITH B = 99.0

$T \times 10^3$	Z	$T \times 10^3$	Z		$T \times 10^3$	Z
1.00	0.104	41.00	0.502		149.00	0.851
6.00	0.205	62.00	0.601	16	161.00	0.874
13.00	0.302	89.00	0.700			
25.00	0.402	126.00	0.800			

TABLE 24

SOLUTION OF FICK'S LINEAR ISOTHERM FOR DIFFUSION INTO A PLATELET (B = 0.0)

$T \times 10^3$	Z	$T \times 10^3$	Z	$T \times 10^3$	Z
5.0	0.080	30.0	0.196	2.40	0.554
10.0	0.113	60.0	0.277		
20.0	0.159	120.0	0.391		

TABLE 25

SOLUTION OF THE PARABOLIC LAW FOR DIFFUSION INTO A PLATELET ($B \rightarrow \infty$)

$T \times 10^3$	Z	$T \times 10^3$	Z	$T \times 10^3$	Z
5.0	0.100	125.0	0.500	405.0	0.900
20.0	0.200	180.0	0.600	500.0	1.000
45.0	0.300	245.0	0.700		
80.0	0.400	320.0	0.800		

TABLE 26

NUMERICAL SOLUTION FOR DIFFUSION INTO A PLATELET WITH B = 0.0

$T \times 10^3$	Z	$T \times 10^3$	Z	$T \times 10^3$	Z
10.0	0.115	195.0	0.504	815.0	0.909
35.0	0.212	280.0	0.602	1080.0	0.950
75.0	0.310	390.0	0.701	1350.0	0.975
125.0	0.402	545.0	0.800	1610.0	0.987

TABLE 27

NUMERICAL SOLUTION FOR DIFFUSION INTO A PLATELET WITH B = 1.0

$T \times 10^3$	Z	$T \times 10^3$	Z	$T \times 10^3$	Z
10,0	0.123	240.0	0.607	880.0	0.976
30.0	0.212	320.0	0.701	1200.0	0.995
60.0	0.300	430.0	0.804	1860.0	1.000
110.0	0.407	590.0	0.901		
170.0	0.508	740.0	0.951		

TABLE 28

NUMERICAL SOLUTION FOR DIFFUSION INTO A PLATELET WITH B = 5.0

$T \times 10^3$	Z	$T \times 10^3$	Z	$T \times 10^3$	Z
6.0	0.103	204.0	0.600	573.0	0.975
24.0	0.206	276.0	0.703	687.0	0.995
54.0	0.308	354.0	0.802	792.0	0.999
93.0	0.405	450.0	0.902		
144.0	0.504	519.0	0.951		

TABLE 29

NUMERICAL SOLUTION FOR DIFFUSION INTO A PLATELET
WITH B = 25.0

$T \times 10^3$	Z	$T \times 10^3$	Z	$T \times 10^3$	Z
5.2	0.100	130.0	0.501	406.9	0.901
20.8	0.200	187.2	0.601	434.2	0.935
46.8	0.300	254.8	0.701		
83.2	0.401	331.5	0.801		

TABLE 30

NITROGEN ADSORPTION ON EVACUATED TYPE 4A PELLETS (1/16") AT -78°C and 1.0 ATMOSPHERE

t,min	Q,cc/g	t,min	Q,cc/g	t,min	Qcc/g
0.5	6.09	9.0	32.16	55.0	57.49
1.0	9.95	10.0	33.66	61.0	58.56
1.5	12.64	11.0	34.84	69.0	59.86
2.0	15.00	13.0	37.16	75.0	60.50
2.5	17.04	16.0	40.06	82.0	61.15
3.0	18.54	20.0	43.38	92.0	61.99
3.5	20.36	25.0	46.90	130.0	63.42
4.0	21.65	30.0	49.58	149.0	63.88
5.0	24.76	36.0	52.37	161.0	64.00
6.0	27.33	41.0	54.21	173.0	64.09
7.0	28.73	46.0	55.19	185.0	64.09
8.0	30.66	49.0	56.19	192.0	64.14

TABLE 31

NITROGEN DESORPTION ON TYPE 4A PELLETS (1/16")
FROM 1.0 ATMOSPHERE TO 0.50 ATMOSPHERE AT -78°C

t,min	Q,cc/g	t,min	Q,cc/g	t,min	Q,cc/g
0.5	63.45	5.0	61.73	20.0	59.84
1.0	63.34	6.0	61.53	25.0	59.47
1.5	63.02	7.0	61.36	35.0	58.88
2.0	62.76	8.0	61.21	43.0	58.41
2.5	62.54	9.0	60.99	104.0	57.68
3.0	62.33	10.0	60.89	117.0	57.66
3.5	62.16	13.0	60.30	124.0	57.66
4.0	61.95	16.0	59.93		

TABLE 32

NITROGEN ADSORPTION ON TYPE 4A PELLETS (1/16")
FROM 0.50 ATMOSPHERE TO 0.75 ATMOSPHERE AT -78°C

t,min	Q,cc/g	t,min	Q,cc/g	t,min	Q,cc/g
0.5	57.95	4.0	58.94	57.0	61.04
1.0	58.12	5.0	59.10	66.0	61.04
1.5	58.12	7.0	59.35	90.0	61.11
2.0	58.36	10.0	59.67	100.0	61.11
2.5	58.53	19.0	60.58	101.0	61.17
3.0	58.61	33.0	60.68		
3.5	58.78	40.0	60.84		

TABLE 33

NITROGEN DESORPTION ON TYPE 4A PELLETS (1/16")
FROM 0.75 ATMOSPHERE TO 0.25 ATMOSPHERE AT -78°C

t,min	Q,cc/g	t,min	Q,cc/g	t,min	Q,cc/g
1.0	59.43	5.0	56.74	32.0	51.45
1.5	58.88	6.0	56.23	36.0	51.20
2.0	58.36	7.0	55.80	48.0	50.53
2.5	58.04	9.0	55.17	49.0	50.53
3.0	57.74	12.0	54.36	60.0	50.08
3.5	57.44	16.0	53.41	67.0	49.88
4.0	57.23	20.0	52.82	76.0	49.69
4.5	56.91	25.0	52.20	94.0	49.69

TABLE 34

NITROGEN ADSORPTION ON EVACUATED TYPE 4A COMPRESSED POWDER AT 1 atm and -78°C

t,min	Q,cc/g	t,min	Q,cc/g	t,min	Q,cc/g
0.5	11.89	10.0	46.31	29.0	61.23
1.0	18.06	11.0	47.61	31.0	61.51
1.5	22.66	12.0	48.67	33.0	62.43
2.0	26.47	13.0	49.98	34.0	62.82
2.5	28.48	14.0	50.91	36.0	63.34
3.0	30.99	15.0	51.82	39.0	64.40
3.5	32.95	16.0	52.67	41.0	65.05
4.0	34.69	17.0	53.69	48.0	66.63
4.5	36.41	18.0	54.68	50.0	67.18
5.0	37.98	19.0	55.25	56.0	68.28
5.5	38.63	20.0	56.04	70.0	70.30
6.0	39.69	21.0	56.58	88.0	71.77
6.5	40.60	22.0	57.10	98.0	72.16
7.0	41.53	24.0	58.49	133.0	73.48
7.5	42.58	25.0	58.99	150.0	73.74
8.5	43.49	26.0	59.66	160.0	73.84
9.0	44.91	27.0	60.18	172.0	73.84

TABLE 35

NITROGEN DESORPTION ON TYPE 4A COMPRESSED POWDER FROM 1 atm to 0.5 atm at -78°C

t,min	Q,cc/gm	t,min	Q,cc/gm	t,min	Q,cc/gm
0.5	72.90	9.0	69.01	45.0	66.87
1.0	72.11	11.0	68.95	62.0	66.40
1.5	71.12	13.0	68.62	107.0	65.99
2.0	71.33	15.0	68.23	116.0	65.99
3.0	70.92	18.0	67.90	120.0	65.99
4.0	70.53	21.0	67.90	171.0	65.88
5.0	70.14	25.0	67.44	182.0	65.60
6.0	69.81	28.0	67.18	190.0	65.60
7.0	69.74	32.0	67.18	196.0	65.60
8.0	69.35	36.0	66.84	207.0	65.54

TABLE 36

NITROGEN DESORPTION ON TYPE 4A COMPRESSED POWDER FROM 1 atm to 0.25 atm at -78°C

t,min	Q,cc/gm	t,min	Q,cc/gm	t,min	Q,cc/gm
0.5	71.49	12.0	62.27	40.0	57.36
1.0	70.59	13.0	62.01	43.0	57.11
1.5	69.78	15.0	61.47	46.0	56.82
2.0	69.01	16.0	61.20	50.0	56.52
2.5	68.39	17.0	60.92	53.0	56.49
3.0	67.90	18.0	60.68	58.0	56.26
3.5	67.38	20.0	60.19	64.0	56.00
4.0	66.82	22.0	59.76	74.0	55.94
4.5	66.53	24.0	59.50	94.0	55.64
5.0	66.03	25.0	59.30	111.0	55.55
6.0	65.47	27.0	59.20	129.0	55.55
7.0	64.69	29.0	58.52	138.0	55.39
8.0	64.17	31.0	58.26	152.0	55.13
9.0	63.89	34.0	58.00	184.0	54.99
10.0	63.37	37.0	57.52	200.0	55.05

TABLE 37

NITROGEN ADSORPTION ON TYPE 4A COMPRESSED POWDER FROM 0.5 atm to 0.75 atm at -78°C

t,min	Q,cc/gm	t,min	Q,cc/gm	t,min	Q,cc/gm
0.5	66.42	6.0	68.80	30.0	70.44
1.0	66.42	8.0	68.90	39.0	70.94
1.5	67.16	9.0	69.26	50.0	70.99
2.0	67.26	12.0	69.55	59.0	71.28
3.0	67.67	15.0	69.95	92.0	71.30
4.0	68.41	22.0	70.34	1850.0	72.61

TABLE 38

VOLUME ADSORBED AT EQUILIBRIUM OF CO_2 on TYPE 4A COMPRESSED POWDER

Temp, °C	Pressure, atm	Volume Adsorbed/ g Catalyst
-78	0.750	144.60
-78	0.375	143.60
-78	0.175	140.90
0°C	1.00	104.00
0°C	0.75	999.70
0°C	0.50	96.00
0°C	0.25	89.10

TABLE 39

METHANE ADSORPTION ON EVACUATED TYPE 4A PELLETS (1/16") at 1.0 ATMOSPHERE and -78°C

t,min	Q,cc/g	t,min	Q,cc/g	t,min	Q,cc/g
0.5	2.31	66.0	29.70	363.0	62.75
1.0	3.36	74.0	31.86	383.0	63.63
1.5	4.11	89.0	35.01	400.0	64.51
2.0	4.66	102.0	37.45	433.0	65.86
2.5	5.43	110.0	38.96	448.0	66.49
3.0	5.75	141.0	43.44	459.0	66.92
3.5	6.18	157.0	45.73	476.0	67.47
4.0	6.62	168.0	47.14	497.0	67.98
5.0	7.39	177.0	48.23	511.0	67.43
6.0	8.14	188.0	49.50	528.0	68.64
7.0	8.80	204.0	51.13	561.0	69.07
9.0	9.99	223.0	53.01	573.0	69.24
12.0	11.73	260.0	56.13	590.0	69.61
16.0	13.80	278.0	57.43	606.0	70.10
20.0	15.65	291.0	58.30	821.0	72.20
25.0	17.40	306.0	59.30	1200.0	77.48
38.0	21.87	326.0	60.68	1590.0	78.75
43.0	23.61	335.0	61.00		
49.0	25.45	343.0	61.55		

TABLE 40

METHANE DESORPTION ON TYPE 4A PELLETS (1/16")
FROM 1.0 ATMOSPHERE to 0.50 ATMOSPHERE AT
-78°C

t,min	Q,cc/g	t,min	Q,cc/g	t,min	Q,cc/g
0.5	78.93	23.0	77.04	204.0	74.35
1.0	78.82	31.0	76.77	253.0	73.99
2.0	78.65	65.0	75.45	273.0	73.95
4.0	78.44	80.0	75.68	302.0	73.78
5.0	78.39	101.0	75.38	324.0	73.52
7.0	78.12	164.0	74.74	337.0	73.52
15.0	77.47	188.0	74.54		

TABLE 41

METHANE ADSORPTION ON TYPE 4A PELLETS (1/16") FROM 0.50 ATMOSPHERE TO 0.75 ATMOSPHERE AT -78°C

t,min	Q,cc/g	t,min	Q,cc/g	t,min	Q,cc/g
1.0	73.65	16.0	74.77	91.0	76.30
1.5	74.05	20.0	74.93	109.0	76.47
3.0	73.97	25.0	75.09	134.0	76.72
4.0	74.05	36.0	75.50	209.0	76.91
6.0	74.21	46.0	75.57	219.0	76.91
9.0	74.45	57.0	75.82	256.0	77.08
13.0	74.60	68.0	75.98		

TABLE 42

METHANE DESORPTION ON TYPE 4A PELLETS (1/16")
FROM 0.75 ATMOSPHERE to 0.25 ATMOSPHERE AT
-78°C

t,min	Q,cc/g	t,min	Q,cc/g	t,min	Q,cc/g
1.0	75.82	12.0	74.02	101.0	70.02
1.5	75.73	16.0	73.64	109.0	69.91
2.0	75.66	24.0	73.04	123.0	69.62
3.0	75.37	25.0	72.87	135.0	69.48
4.0	75.08	35.0	72.38	153.0	69.04
5.0	74.94	42.0	71.97	217.0	68.26
6.0	74.81	52.0	71.53	228.0	68.13
7.0	74.62	64.0	71.03	238.0	68.13
8.0	74.39	71.0	73.29	385.0	67.67
9.0	74.28	95.0	70.16		

TABLE 43

METHANE ADSORPTION ON EVACUATED TYPE 4A COMPRESSED POWDER AT 1.0 ATMOSPHERE AND -78°C

t,min	Q,cc/gm	t,min	Q,cc/gm	t,min	Q,cc/gm
1.0	1.37	83.0	23.84	1195.0	76.46
2.5	1.89	86.0	24.54	1332.0	77.05
4.0	2.54	92.0	24.87	1346.0	77.08
5.0	3.20	95.0	26.06	1379.0	77.25
6.0	3.59	98.0	26.37	1405.0	77.64
6.5	4.11	100.0	27.15	1435.0	77.60
8.0	4.63	232.0	42.94	1465.0	77.73
9.0	5.15	236.0	43.54	1650.0	77.82
12.0	6.84	267.0	46.53	1695.0	78.61
17.0	7.75	310.0	49.81	1762.0	78.53
18.0	8.42	330.0	51.27	1822.0	78.66
22.0	9.98	349.0	52.17	2517.0	78.38
25.0	11.02	382.0	54.13	2543.0	78.74
27.0	11.77	543.0	62.03	2601.0	79.57
29.0	12.03	1028.0	73.47	2639.0	79.71
30.0	12.42	1029.0	75.70	2816.0	79.97
32.0	12.88	1045.0	74.78	2847.0	80.00
35.0	13.85	1056.0	75.87	2958.0	60.10
43.0	15.93	1073.0	75.00	3184.0	80.44
45.0	16.32	1092.0	75.33	3242.0	80.44
50.0	16.83	1103.0	75.40		
60.0	19.43	1151.0	75.78		
74.0	22.15	1172.0	76.08		

TABLE 44

METHANE DESORPTION ON TYPE 4A COMPRESSED POWDER
FROM 1.0 to 0.75 ATMOSPHERE AT -78°C

t,min	Q,cc/gm	t,min	Q,cc/gm	t,min	Q,cc/gm
1.0	79.54	74.0	78.47	273.0	77.07
7.0	79.35	84.0	78.38	473.0	76.23
17.0	79.13	119.0	78.14	1029.0	75.74
32.0	78.96	146.0	77.95		
47.0	78.73	225.0	77.33		

TABLE 45

METHANE DESORPTION ON TYPE 4A COMPRESSED POWDER
FROM 0.75 to 0.50 ATMOSPHERES AT -78°C

t,min	Q,cc/g	t,min	Q,cc/g	t,min	Q,cc/g
2.0	75.14	75.0	73.21	1018.0	70.68
5.0	75.07	101.0	73.16	1054.0	71.64
21.0	74.75	200.0	72.56	1132.0	71.47
40.0	73.87	292.0	72.34	1227.0	71.02
59.0	73.65	295.0	71.98	1647.0	70.42

TABLE 46

METHANE DESORPTION ON TYPE 4A COMPRESSED POWDER
FROM 0.50 to 0.25 ATMOSPHERES AT -78°C

t,min	Q,cc/g	t,min	Q,cc/g	t,min	Q,cc/g
1.0	70.23	68.0	68.02	146.0	66.74
7.0	70.17	72.0	68.02	167.0	66.58
13.0	69.81	87.0	67.84	178.0	66.51
30.0	68.90	99.0	67.68	840.0	64.37
40.0	68.75	113.0	67.28	848.0	64.34
49.0	68.62	124.0	67.13	945.0	64.34

TABLE 47

METHANE ADSORPTION ON EVACUATED TYPE 4A COMPRESSED POWDER AT 0°C and 1 ATMOSPHERE

t,min	Q,cc/g	t,min	Q,cc/g	t,min	Q,cc/g
1.0	4.64	11.0	18.65	48.0	25.91
1.5	6.59	12.0	19.23	53.0	26.42
2.0	7.91	13.0	19.82	82.0	27.01
2.5	9.09	14.0	20.49	99.0	27.34
3.0	10.27	15.0	21.02	116.0	26.94
3.5	10.79	17.0	21.56	141.0	26.98
4.0	11.84	18.0	22.18	188.0	27.33
4.5	12.36	20.0	22.58	213.0	27.18
5.0	12.88	21.0	22.70	238.0	27.46
6.0	14.46	22.0	22.96	249.0	27.49
7.0	15.11	24.0	23.57	262.0	27.46
7.5	16.04	27.0	24.07	291.0	27.40
8.0	16.17	32.0	24.68	303.0	27.46
9.0	17.21	37.0	25.42	843.0	27.67
9.5	18.00	42.0	25.61		

TABLE 48

METHANE DESORPTION ON TYPE 4A COMPRESSED POWDER
FROM 1 ATMOSPHERE TO 0.75 ATMOSPHERE AT 0°C

t,min	Q,cc/g	t,min	Q,cc/g	t,min	Q,cc/g
0.5	26.71	10.0	23.84	40.0	22.28
1.5	26.07	13.0	23.45	63.0	22.25
3.5	25.19	24.0	22.90	533.0	21.63
6.0	24.44	31.0	22.51	1500.0	21.30

TABLE 49

METHANE DESORPTION ON TYPE 4A COMPRESSED POWDER FROM 0.67 ATMOSPHERE to 0.50 ATMOSPHERE AT 0°C

t,min	Q,cc/g	t,min	Q,cc/g	t,min	Q,cc/g
0.5	19.40	7.0	17.63	78.0	15.82
1.0	19.33	10.0	17.18	114.0	15.72
1.5	18.96	12.0	17.13	135.0	15.63
2.0	18.88	13.0	17.63	194.0	15.70
2.5	18.49	20.0	16.71	300.0	14.57
5.0	18.36	31.0	16.04	1090.0	14.88
6.5	17.96	46.0	16.21		

TABLE 50

METHANE DESORPTION ON TYPE 4A COMPRESSED POWDER
FROM 0.5 ATMOSPHERE TO 0.25 ATMOSPHERE AT 0°C

t,min	Q,cc/g	t,min	Q,cc/g	t,min	Q,cc/g
0.5	14.29	9.0	10.89	59.0	8.31
1.0	13.94	10.5	10.44	70.0	8.31
1.5	13.61	13.0	10.21	92.0	7.92
2.0	13.33	15.0	9.90	110.0	8.07
2.5	13.03	18.0	9.62	135.0	8.21
3.0	12.72	20.0	9.37	150.0	8.17
3.5	12.43	23.0	9.34	176.0	8.08
4.5	12.13	28.0	9.02	205.0	7.89
5.5	11.80	36.0	8.72	240.0	7.88
6.5	11.49	42.0	8.66	308.0	7.29
7.5	11.19	49.0	8.31		

TABLE 51

METHANE ADSORPTION ON EVACUATED TYPE 4A COMPRESSED POWDER AT 30°C and 1.0 ATMOSPHERE

t,min	Q,cc/g	t,min	Q,cc/g	t,min	Q,cc/g
1.0	5.16	4.5	10.56	16.0	13.74
1.5	6.59	5.0	11.09	35.0	14.03
2.0	7.91	6.0	11.61	44.0	14.42
2.5	8.56	7.0	11.97	56.0	14.56
3.0	9.35	8.0	12.38	70.0	14.37
3.5	9.90	8.5	12.77	72.0	14.61
4.0	10.29	11.0	13.42		

TABLE 52

METHANE DESORPTION ON TYPE 4A COMPRESSED POWDER
FROM 1.0 ATMOSPHERE TO 0.75 ATMOSPHERE at 30°C

t,min	Q,cc/g	t,min	Q,cc/g	t,min	Q,cc/g
0.5	12.83	4.0	11.52	60.0	10.54
1.0	12.72	7.0	11.13	74.0	10.61
1.5	12.33	29.0	10.69	90.0	10.66
2.0	11.91	45.0	10.67		

TABLE 53

METHANE DESORPTION ON TYPE 4A COMPRESSED POWDER
FROM 0.75 ATMOSPHERE TO 0.50 ATMOSPHERE AT 30°C

t,min	Q,cc/g	t,min	Q,cc/g	t,min	Q,cc/g
1.0	9.92	5.0	8.39	31.0	7.72
1.5	9.53	7.0	8.33	37.0	7.72
2.0	9.12	8.0	8.00	607.0	7.71
3.0	8.86	11.0	8.00		
4.0	8.72	17.0	7.72		

TABLE 54

METHANE DESORPTION ON TYPE 4A COMPRESSED POWDER
FROM 0.5 ATMOSPHERE TO 0.25 ATMOSPHERE AT 30°C

t,min	Q,cc/g	t,min	Q,cc/g	t,min	Q,cc/g
0.5	6.82	3.5	5.26	48.0	4.15
1.0	6.48	5.0	4.96	95.0	3.90
1.5	6.15	6.0	4.67	116.0	3.93
2.0	5.84	13.0	4.38	125.0	3.96
2.5	5.55	27.0	4.14	141.0	3.92

TYPE 55

METHANE ADSORPTION ON EVACUATED TYPE 4A COMPRESSED POWDER AT 50°C and 1.0 ATMOSPHERE

t,min	Q,cc/g	t,min	Q,cc/g	t,min	Q,cc/g
1.0	5.22	3.0	7.81	7.5	9.11
1.5	6.39	3.5	8.20	12.0	9.24
2.0	6.91	5.0	8.72	23.0	9.34
2.5	7.30	6.0	8.85	34.0	9.35

TABLE 56

METHANE DESORPTION ON TYPE 4A COMPRESSED POWDER FROM 1.0 ATMOSPHERE to 0.50 ATMOSPHERE AT 50°C

t,min	Q,cc/g	t,min	Q,cc/g	t,min	Q,cc/g
0.5	7.58	2.5	5.94	23.0	5.03
1.0	7.11	4.0	5.49	30.0	5.03
1.5	6.72	8.5	5.10	70.0	5.00
2.0	6.33	14.0	5.03		

TABLE 57

METHANE ADSORPTION ON TYPE 4A COMPRESSED POWDER
FROM 0.33 ATMOSPHERE TO 0.75 ATMOSPHERE AT 50°C

t,min	Q,cc/g	t,min	Q,cc/g	t,min	Q,cc/g
0.5	5.23	2.5	6.91	13.0	7.68
1.0	5.73	4.0	7.30	46.0	7.66
1.5	6.13	7.0	7.30		
2.0	6.52	10.0	7.58		

TABLE 58

METHANE DESORPTION ON TYPE 4A COMPRESSED POWDER FROM 0.50 ATMOSPHERE TO 0.25 ATMOSPHERE AT 50°C

t,min	Q,cc/g	t,min	Q,cc/g	t,min	Q,cc/g
0.5	4.40	3.0	3.28	30.0	2.24
1.0	4.02	7.0	2.89	46.0	1.84
1.5	3.69	13.0	2.72		
2.0	3.59	21.0	2.36		

TABLE 59

ETHANE ADSORPTION ON EVACUATED TYPE 4A COMPRESSED POWDER AT 1.0 ATMOSPHERE AND -78°C *

t,min	Q,cc/g	t,min	Q,cc/g	t,min	Q,cc/g
0.5	1.23	121.0	7.17	1930.0	26.56
2.0	1.20	147.0	8.04	2020.0	27.21
4.0	1.19	161.0	8.72	2537.0	30.61
5.5	1.37	176.0	9.02	2574.0	30.68
9.5	1.60	187.0	9.57	2634.0	31.01
10.5	1.86	295.0	11.91	2677.0	31.45
40.0	3.54	329.0	12.56	2732.0	31.84
41.0	3.63	374.0	13.09	2841.0	32.36
46.0	3.83	409.0	13.68	2965.0	33.57
52.0	4.06	461.0	14.52	3157.0	33.82
59.0	4.50	490.0	14.78	3277.0	34.17
65.0	4.86	1177.0	22.60	3367.0	34.72
72.0	5.23	1192.0	22.56	3983.0	37.32
84.0	5.62	1392.0	23.63	4022.0	37.46
90.0	6.01	1412.0	23.57	4132.0	37.52
97.0	6.17	1520.0	24.40	4177.0	38.00
102.0	6.41	1637.0	24.96	4303.0	38.98
112.0	7.06	1715.0	25.04	4378.0	39.40
120.0	6.93	1880.0	25.65		

* Leak started in Equipment after 4378 minutes.

TABLE 60

ETHANE ADSORPTION ON EVACUATED TYPE 4A COMPRESSED POWDER AT 1.0 ATMOSPHERE AND 0°C

t,min	Q,cc/g	t,min	Q,cc/g	t,min	Q,cc/g
0.5	4.09	10.5	31.00	33.0	48.58
1.0	6.84	11.0	31.65	34.0	49.00
1.5	8.42	11.5	32.11	38.0	50.38
2.0	11.63	12.5	33.41	43.0	51.82
2.5	13.46	13.0	34.20	47.0	52.72
3.0	15.30	13.5	34.56	56.0	54.37
3.5	16.87	14.0	35.34	63.0	55.38
4.0	18.36	15.0	36.12	72.0	56.13
4.5	19.81	16.0	37.29	84.0	57.04
5.0	20.99	19.0	40.12	98.0	57.69
5.5	22.01	20.0	40.64	104.0	57.81
6.0	23.18	21.0	41.56	137.0	58.27
6.5	24.10	22.0	42.34	151.0	58.43
7.0	25.14	25.0	44.23	167.0	58.65
7.5	26.20	26.0	45.01	816.0	59.41
8.0	27.11	27.0	45.53	822.0	59.53
9.5	29.55	28.0	46.04		
10.0	30.22	30.0	47.02		

TABLE 61

ETHANE DESORPTION ON TYPE 4A COMPRESSED POWDER FROM 1.0 ATMOSPHERE TO 0.50 ATMOSPHERE AT 0°C

t,min	Q,cc/g	t,min	Q,cc/g	t,min	Q,cc/g
0.5	58.88	8.0	57.71	26.0	57.33
1.0	58.80	11.0	57.62	35.0	57.17
1.5	58.54	14.0	57.50	43.0	57.14
3.0	58.18	18.0	57.34	54.0	57.03

TABLE 62

ETHANE DESORPTION ON TYPE 4A COMPRESSED POWDER FROM 0.50 ATMOSPHERE TO 0.25 ATMOSPHERE AT 0°C

t,min	Q,cc/g	t,min	Q,cc/g	t,min	Q,cc/g
1.0	56.33	10.0	54.83	39.0	53.98
2.0	56.03	17.0	54.52	42.0	53.98
3.0	55.72	23.0	54.24	92.0	53.98
5.0	55.39	32.0	54.28	113.0	53.92

TABLE 63

ETHANE ADSORPTION ON TYPE 4A COMPRESSED POWDER
FROM 0.25 ATMOSPHERE TO 0.75 ATMOSPHERE AT 0°C

t,min	Q,cc/g	t,min	Q,cc/g	t,min	Q,cc/g
1.0	54.58	5.0	56.19	14.5	57.36
1.5	54.87	6.0	56.38	20.5	57.56
2.0	55.26	7.0	56.58	43.0	58.01
2.5	55.57	10.0	56.97	53.0	58.05
3.5	55.75	11.0	57.07	91.0	57.92
4.0	55.96	11.5	57.16		

TABLE 64

ETHANE ADSORPTION ON EVACUATED TYPE 4A COMPRESSED POWDER AT 0.87 ATMOSPHERE AND 30°C

t,min	Q,cc/g	t,min	Q,cc/g	t,min	Q,cc/g
1.5	14.21	12.0	39.31	93.0	49.41
2.0	17.06	14.0	40.90	109.0	49.52
2.5	19.56	17.0	42.61	124.0	49.75
3.0	21.83	19.0	43.48	183.0	49.94
4.0	25.59	24.0	45.65	238.0	49.98
5.0	28.21	26.0	47.44	243.0	50.09
6.0	30.83	33.0	48.22	298.0	50.23
7.0	32.65	48.0	48.63	344.0	50.23
8.0	34.35	59.0	49.07	484.0	50.64
9.0	36.06	73.0	49.29	514.0	50.61
10.0	37.20	85.0	49.41		

TABLE 65

ETHANE ADSORPTION ON TYPE 4A COMPRESSED POWDER FROM 0.87 ATMOSPHERES TO 1.0 ATMOSPHERES at 30°C

t,min	Q,cc/g	t,min	Q,cc/g	t,min	Q,cc/g
0.5	51.03	62.0	51.69	827.0	52.25
5.5	51.42	77.0	51.62	866.0	52.11
11.0	51.43	118.0	51.71		
26.0	51.56	169.0	51.81		

TABLE 66

ETHANE DESORPTION ON TYPE 4A COMPRESSED POWDER FROM 1.0 ATMOSPHERE TO 0.50 ATMOSPHERE AT 30°C

t,min	Q,cc/g	t,min	Q,cc/g	t,min	Q,cc/g
0.5	50.16	4.0	48.52	66.0	46.60
1.0	50.01	4.5	48.29	87.0	46.47
1.5	49.65	5.5	48.02	102.0	46.54
2.0	49.32	8.5	47.64	124.0	46.53
2.5	49.06	12.0	47.31	159.0	46.46
3.0	48.78	19.0	46.96	199.0	46.38
3.5	48.60	41.0	46.62	329.0	46.44

TABLE 67

ETHANE DESORPTION ON TYPE 4A COMPRESSED POWDER FROM 0.50 ATMOSPHERE TO 0.25 ATMOSPHERE AT 30°C

t,min	Q,cc/g	t,min	Q,cc/g	t,min	Q,cc/g
0.5	44.26	7.0	41.24	54.0	39.37
1.0	43.80	8.0	41.03	81.0	39.33
1.5	43.39	9.0	40.88	99.0	39.30
2.0	42.94	12.0	40.50	131.0	39.24
3.0	42.41	17.0	40.14	150.0	39.17
4.0	42.00	22.0	39.76	711.0	39.04
5.0	41.80	30.0	39.59		
6.0	41.44	44.0	39.57		

TABLE 68

ETHANE ADSORPTION ON EVACUATED TYPE 4A COMPRESSED POWDER AT 00.50 ATMOSPHERE AND 30°C

t,min	Q,cc/g	t,min	Q,cc/g	t,min	Q,cc/g
1.0	7.97	10.5	30.54	43.0	41.50
1.5	9.82	11.0	31.06	50.0	42.08
2.0	13.14	11.5	31.59	58.0	42.67
2.5	15.07	12.0	32.04	69.0	43.12
3.0	16.66	12.5	32.34	78.0	43.49
3.5	18.31	13.0	32.94	96.0	43.88
4.0	19.90	14.0	33.47	109.0	44.06
4.5	20.99	15.0	34.09	122.0	44.26
5.0	22.05	16.0	34.79	137.0	44.36
5.5	23.05	17.0	35.34	164.0	44.66
6.0	24.18	18.0	35.87	174.0	44.59
6.5	24.96	19.0	36.29	253.0	44.91
7.0	25.82	20.0	36.70	287.0	45.03
7.5	26.82	21.0	37.09	320.0	45.17
8.0	27.34	23.0	37.82	363.0	45.20
8.5	27.99	25.0	38.55	391.0	45.26
9.0	28.80	27.0	39.13	585.0	45.56
9.5	29.34	31.0	39.88	691.0	45.84
10.0	30.00	36.0	40.76	811.0	46.30

TABLE 69

ETHANE ADSORPTION ON EVACUATED TYPE 4A COMPRESSED POWDER AT 1.0 ATMOSPHERE AND 50°C

t,min	Q,cc/g	t,min	Q,cc/g	t,min	Q,cc/g
1.0	12.15	8.5	35.51	41.0	42.96
1.5	16.80	9.0	35.77	47.0	43.15
2.0	19.92	9.5	36.41	59.0	43.43
2.5	22.41	10.0	36.80	70.0	43.56
3.0	24.38	10.5	37.32	82.0	43.49
3.5	26.07	11.0	37.59	90.0	43.65
4.0	27.65	12.0	38.11	100.0	43.70
5.0	29.81	13.0	38.76	104.0	43.80
5.5	30.87	17.0	40.25	208.0	44.09
6.0	31.75	20.0	40.76	230.0	44.37
6.5	32.79	24.0	41.61	247.0	44.33
7.0	33.54	25.0	41.90	267.0	44.30
7.5	34.33	31.0	42.26		
8.0	34.85	38.0	42.71		

TABLE 70

ETHANE DESORPTION ON TYPE 4A COMPRESSED POWDER FROM 1.0 ATMOSPHERE TO 0.50 ATMOSPHERE AT 50°C

t,min	Q,cc/g	t,min	Q,cc/g	t,min	Q,cc/g
0.5	41.90	4.5	38.74	77.0	34.99
1.0	40.93	6.0	38.39	78.0	36.75
1.5	40.54	7.0	38.13	105.0	36.74
2.0	40.15	11.0	37.55	123.0	36.65
2.5	39.50	21.0	37.42	653.0	36.84
3.0	39.44	30.0	26.71	679.0	36.51
3.5	39.11	46.0	36.06		

TABLE 71

ETHANE DESORPTION ON TYPE 4A COMPRESSED POWDER FROM 0.50 ATMOSPHERE TO 0.25 ATMOSPHERE AT 50°C

t,min	Q,cc/g	t,min	Q,cc/g	t,min	Q,cc/g
1.0	34.22	5.5	30.87	14.0	28.63
1.5	33.68	6.0	30.68	19.0	28.35
2.0	33.08	6.5	30.41	21.0	28.05
2.5	32.50	7.0	30.38	30.0	27.82
3.0	32.34	7.5	30.10	37.0	27.79
3.5	32.04	8.5	29.73	46.0	27.56
4.0	31.74	9.5	29.45	61.0	27.59
5.0	31.14	11.0	29.12		

TABLE 72

ETHANE ADSORPTION ON TYPE 4A COMPRESSED POWDER FROM 0.50 ATMOSPHERE TO 0.75 ATMOSPHERE AT 50°C

t,min	Q,cc/g	t,min	Q,cc/g	t,min	Q,cc/g
0.5	37.52	3.0	39.30	87.0	41.16
1.0	37.91	5.0	39.69	93.0	41.12
1.5	38.30	6.5	40.00	106.0	41.12
2.0	38.71	18.0	40.69		
2.5	39.00	52.0	40.99		

TABLE 73

ETHANE ADSORPTION ON EVACUATED TYPE 4A COMPRESSED POWDER AT 0.50 ATMOSPHERE AND 50°C

t,min	Q,cc/g	t,min	Q,cc/g	t,min	Q,cc/g
1.0	8.31	8.0	24.28	38.0	32.81
1.5	10.95	8.5	24.80	44.0	33.00
2.0	12.97	9.0	25.20	52.0	33.53
2.5	14.76	10.0	26.04	60.0	33.76
3.0	16.34	11.0	26.84	72.0	34.17
3.5	17.64	12.0	27.36	95.0	34.60
4.0	18.10	13.0	27.89	126.0	34.66
4.5	19.68	15.0	28.92	153.0	34.80
5.0	20.53	16.0	29.18	210.0	35.11
5.5	21.43	17.0	29.44	238.0	35.31
6.0	22.08	18.0	29.74	278.0	35.44
6.5	22.87	22.0	30.67	806.0	36.51
7.0	23.39	25.0	31.27	864.0	36.51
7.5	24.02	32.0	32.01		

APPENDIX II

Check of Computer Program.

If theoretical equations are not available to check the results of the computer program, then a change in the number of intervals into which the particle is subdivided can be examined. For example, if the equations based on finite difference methods in the computer program are correct then a change from 21 to 11 intervals will not change the results. This was done in the case of the sphere and the results are shown in Figure 42. The agreement between the results based on 21 and 11 intervals is very close.

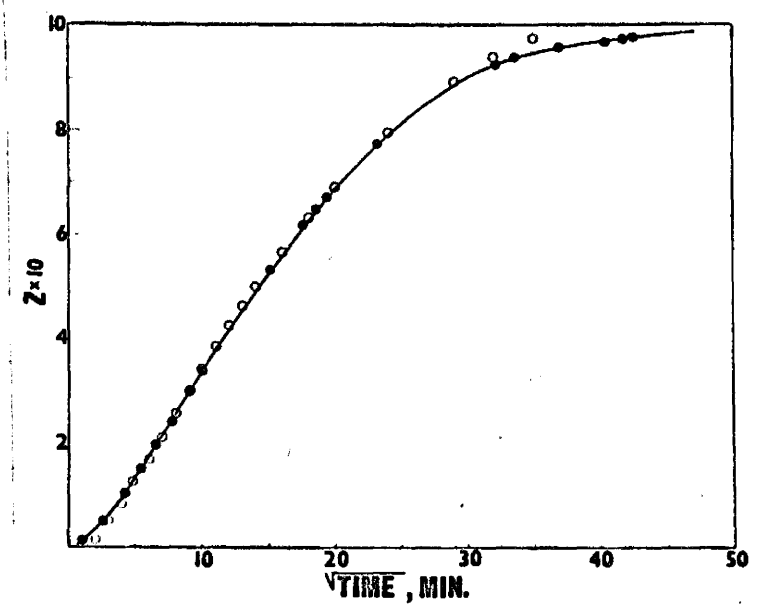

FIGURE 42:
Comparison of Change of Number of Intervals in the Computer Program as Z versus $T^{\frac{1}{2}}$ for the Sphere at B = 0.0.
0 : 11 intervals
0 : 21 intervals

APPENDIX III

Reproducibility of Experimental Results.

This section is concerned with the reproducibility of the experimental results. Runs were repeated through the experimental portion and Figure 43 is typical of the results. The agreement is very close as shown for Ethane adsorption on Type 4A compressed powder at 0°C and 1 atm. The experimental readings were always within 0.1 cc.

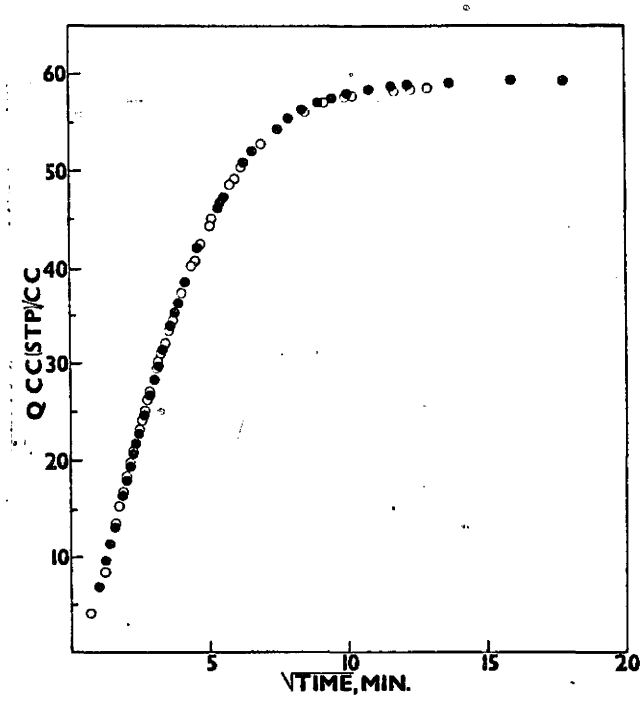

FIGURE 43:
Check on the Reproducibility of Experimental Results as Q versus $\sqrt{\text{Time}}$ for Ethane on Type 4A Compressed Powder at 1 atm. and 0°C.

0 : Original Experiment
0 : Check